

Dynamical Systems: Some Computational Problems

John Guckenheimer* and Patrick Worfolk*
 Center for Applied Mathematics
 504 Engineering and Theory Center
 Cornell University
 Ithaca, NY 14853
 USA

Abstract

We present several topics involving the computation of dynamical systems. The emphasis is on work in progress and the presentation is informal – there are many technical details which are not fully discussed. The topics are chosen to demonstrate the various interactions between numerical computation and mathematical theory in the area of dynamical systems. We present an algorithm for the computation of stable manifolds of equilibrium points, describe the computation of Hopf bifurcations for equilibria in parametrized families of vector fields, survey the results of studies of codimension two global bifurcations, discuss a numerical analysis of the Hodgkin and Huxley equations, and describe some of the effects of symmetry on local bifurcation.

1 Introduction

This article is a written record of the lectures delivered at the 1992 NATO Summer School in Montreal. The spirit of the lectures was informal, and we have tried to preserve the informality and didactic quality of the lectures. The lectures dealt with several related topics, all involving computations of dynamical systems. The emphasis here stresses topics that have not yet been fully developed in other recent papers. Accordingly, they reflect to a large extent “work in progress” rather than presenting a summary and review that makes a finished mathematical tale. There is also a lack of rigor that reflects a pragmatic approach that seeks reliable answers to questions even when these answers cannot be totally integrated into formal mathematical theory.

Our goal is to answer questions about specific dynamical systems. If $f : R^n \times R^k \rightarrow R^n$ defines a k parameter family of vector fields, we would like to know everything about the phase portraits of f and the bifurcations that occur as parameters are varied. Since most dynamical systems cannot be integrated in terms of analytic expressions that are valid for all time, this is a task that can only be approached sensibly through numerical computation. This is problematic for mathematicians because naive error estimates tend to grow exponentially with iterative calculations such as the numerical integration of a vector field. For the most part, we ignore this difficulty and proceed with confidence that computers

*Research partially supported by the National Science Foundation.

provide good approximations to trajectories of vector fields. We seek to find additional algorithms that allow us to calculate aspects of dynamical systems that are hard to determine otherwise. Though these lectures do not emphasize applications, our interests extend beyond individual algorithms to the implementation of efficient and powerful problem solving environments for the analysis of dynamical systems and their bifurcations [3].

2 Computing Stable Manifolds of Equilibria

The stable and unstable manifolds of equilibrium points are important geometric objects in the phase portraits of vector fields. The Stable Manifold Theorem asserts their existence, and some proofs of the Stable Manifold Theorem are constructive; e.g. [53]. Nonetheless, the numerical computation of stable and unstable manifolds of dimension larger than one presents difficulties. This section describes some of these difficulties and sketches an approach that leads to a reasonable algorithm for displaying the two-dimensional stable manifold of the Lorenz system [50].

We begin by recalling the Stable Manifold Theorem for equilibria of finite-dimensional vector fields:

Theorem 2.1 *Let X be a C^r vector field on an n -dimensional manifold M with an equilibrium point p and flow Φ . Let $L : T_p(M) \rightarrow T_p(M)$ be the linearization of X at p . Assume that $T_p(M)$ splits as an invariant direct sum $E^s + E^u$ with the spectrum of $L|E^s$ in the open left half plane of \mathbb{C} and the spectrum of $L|E^u$ in the open right half plane of \mathbb{C} . Then there are C^r submanifolds W^s and W^u passing through p with tangent spaces E^s and E^u respectively with the following property:*

$$W^s = \{x \in M | \Phi(t, x) \rightarrow p \text{ as } t \rightarrow \infty\}$$

$$W^u = \{x \in M | \Phi(t, x) \rightarrow p \text{ as } t \rightarrow -\infty\}.$$

If Φ is complete, then W^s and W^u are 1 – 1 immersions of Euclidean spaces into M .

There is a naive approach to computing the stable manifold of an equilibrium that can be derived from the simplest proofs of the Stable Manifold Theorem. If p is an equilibrium point with the linearization at p having stable manifold E^s and unstable manifold E^u , the stable manifold of p can be represented in local coordinates as the graph of a function $\gamma : E^s \rightarrow E^u$. Near p , each affine subspace parallel to E^u intersects W^s in a single point. The function γ has vanishing derivative at p , so points of E^s near p form a good C^1 approximation to W^s there. Using the invariance of the stable manifold, the backwards trajectories starting on a sphere surrounding p in E^s sweep out an approximation to W^s . One can choose a set of initial conditions on E^s and compute their trajectories to visualize W^s , but the process often works poorly.

Let us examine the Lorenz system as an example. The equations of the Lorenz system are

$$\begin{aligned}\dot{x} &= \sigma(y - x) \\ \dot{y} &= \rho x - y - xz \\ \dot{z} &= -\beta z + xy\end{aligned}$$

with “standard” parameters $\sigma = 10$, $\beta = 8/3$, and $\rho = 28$. For these parameters, the origin is a saddle point with a two-dimensional stable manifold and a one-dimensional unstable manifold. The linearization at the origin is given by the matrix

$$\begin{pmatrix} -10 & 10 & 0 \\ 28 & -1 & 0 \\ 0 & 0 & -8/3 \end{pmatrix}.$$

The negative eigenvalues of this matrix are approximately -2.67 and -22.8 with a ratio that is approximately 8.56 . There are two problems associated with the large ratio between these eigenvalues. First, “most” trajectories in the stable manifold approach the origin from directions close to the z axis which is the eigendirection of the eigenvalue $-8/3$. This can be seen readily by solving the linear system

$$\begin{aligned} \dot{x} &= -ax \\ \dot{y} &= -by \end{aligned}.$$

The trajectories of this system lie along the curves $y = cx^{a/b}$. Points uniformly distributed on the unit circle approach the origin with much higher density close to the y axis if $a \ll b$. The second problem is that the trajectories flow much faster in the eigendirection of the eigenvalue of larger magnitude than in the eigendirection of the weaker eigenvalue. A small circle of initial conditions in the stable manifold will flow backwards to an ellipse whose axes have a ratio approximately $e^{8.56} \approx 5220$ after one unit of time. Thus a fixed time integration of the vector field on a set of initial conditions clustered near the weak eigendirection still will yield a set of points that stretches along the strong eigendirection.

This discussion indicates that strategies for drawing stable manifolds based solely upon the numerical integration of trajectories starting from initial values near the equilibrium may be ineffective. To obtain approximations to large regions of a stable manifold, our approach is to mimic the construction of “geodesic coordinates” in differential geometry. We describe the general construction.

Let p be a hyperbolic equilibrium point of a vector field X on a Riemannian manifold M and let $W = W^s(p)$ be the stable manifold of p . We make use of the Riemannian metric induced on W from its embedding in the ambient Riemannian manifold M . There is a neighborhood U of p in W such that $U - \{p\}$ is foliated by spheres S_r which lie at a distance r from p in the Riemannian metric. We would like to write a differential equation for the evolution of these spheres with increasing r , and this is easy to do when the vector field X is not tangent to S_r . The fundamental observation that allows us to proceed is that the tangent space $T_x(W)$ to W at $x \in S_r$ is spanned by X and $T_x(S_r)$ as long as the vector field is not tangent to S_r . The unique geodesic in W from p to any point of the sphere S_r is characterized by the requirement that it is orthogonal to S_r and that its tangent has unit length and lies in the subspace spanned by the tangents to S_r and the vector field X . This provides the motivation for an algorithm to evolve the sphere S_r by extending the geodesics through p and points on the sphere, as pictured in Figure 1.

Theorem 2.2 *Let X be a C^r vector field on an n -dimensional Riemannian manifold M with a hyperbolic equilibrium point p and flow Φ . Let W be the s -dimensional stable manifold*

of p and let S_r be the geodesic sphere at distance r from p in the Riemannian metric induced on W . If X is not tangent to S_r , then the vector field obtained by orthogonally projecting X onto the normal bundle of S_r is tangent to the geodesic rays of W emanating from p .

There may well be tangencies between the vector field X and the geodesic spheres S_r in a stable manifold. When this happens, it is no longer a simple matter to “evolve” S_r as a submanifold without additional geometric information. We approach the problem with the question of determining when does the set of trajectories passing through a submanifold S of initial conditions form a smooth submanifold W . We point out two difficulties. The following example illustrates one problem that occurs if there are isolated points of tangency between X and S .

Let X be the vector field $X = \partial_x - x\partial_y + x^2\partial_z$ in R^3 and let S be the x axis. The vector field X is tangent to S at the origin. The flow of X is defined by the map $\Phi(x, y, z, t) = (x + t, y - xt - t^2/2, z + x^2t + xt^2 + t^3/3)$. The surface of trajectories with initial conditions on the curve S is given by the map $F(x, t) = (x + t, -xt - t^2/2, x^2t + xt^2 + t^3/3)$. The image of F is a singular surface whose intersection with the plane $x = 0$ is a cusp. This example indicates that given a smooth submanifold S of dimension $s - 1$, there are simple vector fields with the property that the trajectories passing through the submanifold do not form a smooth surface of dimension s . Locally, a submanifold S may be evolved by a vector field X in such a fashion, as long as the tangent spaces to S do not contain X . However, at points of tangency additional information is required to ensure that the trajectories through S will form a smooth submanifold.

There is a further difficulty that we encounter in evolving submanifolds. Suppose that W is a submanifold with boundary and that X is a vector field with a segment of a trajectory γ in the boundary of W . Assume that W is contained in the interior of an invariant manifold \hat{W} of the same dimension. It is not true that W and the vector field define \hat{W} . If the trajectory γ never enters the interior of W , then $\hat{W} - W$ may consist of points whose trajectories do not intersect W at all. For example, the most dramatic case occurs when the dimension of W is two and the boundary of W is a periodic orbit. In this case, we cannot “grow” W in the fashion that we wish to use for stable and unstable manifolds. On the other hand, the scenario we have just described cannot occur for a stable or unstable manifold, since these invariant manifolds are formed by a set of trajectories that are asymptotic to an equilibrium point.

This story ends in an unfinished state. We would like to use algorithms based upon computing geodesics for computing stable and unstable manifolds because they display the geometry of the manifolds in a way that naive computation of trajectories does not. On the other hand, there are mathematical difficulties with the formulation of algorithms that are based solely upon the computation of a vector field that will be tangent to geodesics. This is an area of research in which more work is warranted. The goal is to find a procedure that “works” for the largest possible class of examples, where the criterion of success is the ability to carry out the computation to a specified precision in a reasonable amount of time. Figure 2 shows a picture of the computed stable manifold for the origin of the Lorenz system.

3 Computing Hopf Bifurcations

This section describes joint work in progress with Mark Myers and Bernd Sturmfels. The question we discuss involves the computation of points where Hopf bifurcations occur in parametrized families of vector fields. Let $\dot{x} = f_\lambda(x)$ be a system of differential equations on R^n depending upon a k -dimensional parameter λ . One of the first steps in a bifurcation analysis of this family is the determination of parameter values at which there are non-hyperbolic equilibrium points $(x, \lambda) \in R^n \times R^k$. These points are characterized by the conditions that $f_\lambda(x) = 0$ and $Df_\lambda(x)$ has a zero or purely imaginary eigenvalue. In both cases, the set of parameter values at which bifurcation occurs is expected to have codimension one in the parameter space. Generically, the case of a zero eigenvalue is a saddle-node bifurcation while the case of pure imaginary eigenvalues is a Hopf bifurcation [36]. Note that solving the equations describing either type of bifurcation does not involve numerical integration of the differential equations. Instead, one has a root-finding problem to solve. Since the Jacobian $Df_\lambda(x)$ depends upon f , it is not immediately apparent that one can express this problem as a non-degenerate system of $n+1$ equations in $n+k$ variables.

For saddle-node bifurcations, zero eigenvalues of the Jacobian can be detected by computing the determinant of the Jacobian. It is not difficult to prove that the map $F : R^n \times R^k \rightarrow R^{n+1}$ given by $F(x, \lambda) = (f_\lambda(x), \det(Df_\lambda(x)))$ is non-degenerate for generic f at most points [46]. The fundamental example is given by the normal form for a saddle-node bifurcation: $f_\lambda(x) = \lambda + x^2$. In this example, $F(x, \lambda) = (\lambda + x^2, 2x)$ is non-singular. The general saddle-node bifurcation can be transformed to this normal form by using the techniques of singularity theory [32]. In implementing algorithms for computing saddle-node bifurcations, we face questions about the efficiency and accuracy with which the determinant of the Jacobian of a map can be computed.

We seek algorithms that will locate Hopf bifurcations in a manner analogous to the computation of saddle-node bifurcations. Thus, we want a map $H : R^n \times R^k \rightarrow R^{n+1}$ which vanishes when Df has an equilibrium at which there are a pair of pure imaginary eigenvalues. A basic aspect of this problem is finding a criterion for determining when a matrix has a pair of pure imaginary eigenvalues. A complete algebraic solution to this problem is more complex than finding a criterion for zero eigenvalues. The set of matrices with pure imaginary eigenvalues does not define an algebraic hypersurface in the space of matrices, but rather a semialgebraic set. Let us see what this means in concrete terms for 2×2 matrices. A 2×2 matrix has pure imaginary eigenvalues if and only if its trace vanishes and its determinant is positive. Thus the set of 2×2 matrices with pure imaginary eigenvalues is specified by one equation *and* one inequality on the coefficients of the matrix. If we drop the inequality, then we find matrices with real eigenvalues of equal magnitude and opposite sign as well as matrices with pure imaginary eigenvalues.

There are classical algebraic theories that address the question of when a matrix has a pair of pure imaginary eigenvalues. These theories are now best known in the form of the Routh-Hurwitz criteria that a matrix have all of its eigenvalues in the left half plane. We have applied these theories and continuation strategies in order to implement algorithms for computing Hopf bifurcations. Here we give a brief indication of the algebraic foundation for our algorithms that give criteria for a square matrix to have a pair of pure imaginary eigenvalues. For the remainder of this section, we let A denote an $n \times n$ real matrix and

$P(\lambda) = \det(\lambda I - A)$ denote its characteristic polynomial. The roots of P are the eigenvalues of A . There are two approaches to our algebraic problem: To give criteria for the polynomial P to have a pair of pure imaginary roots, or, alternatively, to give criteria for A to have a pair of pure imaginary eigenvalues by performing algebraic transformations directly on A .

We make the basic observation that if a real polynomial P has a pure imaginary root λ , then $-\lambda$ is also a root. Thus a necessary condition for P to have a pair of pure imaginary roots is that the polynomials P and $Q(x) = P(-x)$ have a common root. The *Sylvester resultant* is a function of the coefficients of P and Q that vanishes if and only if P and Q share a common root. Applied in the context of our problem, we first reduce the size of the problem by observing that the polynomials $R = P + Q$ and $S = P - Q$ are even and odd, respectively. Moreover, P and Q have a common root if and only if R and S have a common root. We can write $R(x) = \hat{R}(x^2)$ and $S(x) = x\hat{S}(x^2)$ with \hat{R} and \hat{S} polynomials of degree approximately $n/2$. Therefore, the Sylvester resultant of \hat{R} and \hat{S} gives a function that vanishes if and only if P and Q have a common root or, equivalently, P has two roots whose sum is zero. If we denote

$$P(\lambda) = c_0 + c_1\lambda + \cdots + c_{n-1}\lambda^{n-1} + \lambda^n,$$

and n is even, the Sylvester resultant is the determinant of the matrix

$$S = \left(\begin{array}{cccccccc} c_0 & c_2 & \cdots & c_{n-2} & 1 & 0 & 0 & \cdots & 0 \\ 0 & c_0 & c_2 & \cdots & c_{n-2} & 1 & 0 & \cdots & 0 \\ \vdots & & & & & & & & \vdots \\ 0 & \cdots & \cdots & 0 & c_0 & c_2 & \cdots & c_{n-2} & 1 \\ c_1 & c_3 & \cdots & c_{n-1} & 0 & 0 & \cdots & \cdots & 0 \\ 0 & c_1 & c_3 & \cdots & c_{n-1} & 0 & \cdots & \cdots & 0 \\ \vdots & & & & & & & & \vdots \\ 0 & \cdots & \cdots & 0 & c_1 & c_3 & \cdots & \cdots & c_{n-1} \end{array} \right) \left. \begin{array}{l} \\ \\ \\ \\ \\ \\ \\ \end{array} \right\} \begin{array}{l} \frac{n-2}{2} \text{ rows} \\ \\ \\ \frac{n}{2} \text{ rows} \end{array}$$

while if n is odd, it is the determinant of the matrix

$$S = \left(\begin{array}{cccccccc} c_0 & c_2 & \cdots & c_{n-3} & c_{n-1} & 0 & 0 & \cdots & 0 \\ 0 & c_0 & c_2 & \cdots & c_{n-3} & c_{n-1} & 0 & \cdots & 0 \\ \vdots & & & & & & & & \vdots \\ 0 & \cdots & \cdots & 0 & c_0 & c_2 & \cdots & c_{n-3} & c_{n-1} \\ c_1 & c_3 & \cdots & c_{n-2} & 1 & 0 & \cdots & \cdots & 0 \\ 0 & c_1 & c_3 & \cdots & c_{n-2} & 1 & 0 & \cdots & 0 \\ \vdots & & & & & & & & \vdots \\ 0 & \cdots & \cdots & 0 & c_1 & c_3 & \cdots & c_{n-1} & 1 \end{array} \right) \left. \begin{array}{l} \\ \\ \\ \\ \\ \\ \end{array} \right\} \begin{array}{l} \frac{n-1}{2} \text{ rows} \\ \\ \\ \frac{n-1}{2} \text{ rows} \end{array}.$$

The resultant encodes the outcome of applying the Euclidean algorithm to a pair of polynomials. If two polynomials have a common root, then the Euclidean algorithm yields the greatest common denominator of the two polynomials. The coefficients of this GCD can be expressed as determinants in the coefficients of the two polynomials. These determinants are the subresultants of the two polynomials. These resultants give explicit functions

n	$P(\lambda) = c_0 + c_1\lambda + \dots + c_{n-1}\lambda^{n-1} + \lambda^n$
2	$c_1 = 0, \quad c_0 > 0$
3	$c_0 - c_1c_2 = 0, \quad c_1 > 0$
4	$c_0c_3^2 - c_1c_2c_3 + c_1^2 = 0, \quad c_1c_3 > 0$
5	$(c_2 - c_3c_4)(c_1c_2 - c_0c_3) + c_1c_4(c_1c_4 - 2c_0) + c_0^2 = 0,$ $(c_2 - c_3c_4)(c_0 - c_1c_4) > 0$
6	$c_0c_5^2(c_0c_5 - c_2c_3) + c_1c_5^2(c_2^2 - c_0c_4) + c_1(c_1^2 + c_0c_3c_5) + c_1c_5(c_0c_3 - 2c_1c_2) +$ $(c_4c_5 - c_3)(c_0c_3^2 - c_0c_1c_5 + c_1^2c_4 - c_1c_2c_3) = 0,$ $(c_1c_3 + c_0c_5^2 - c_1c_4c_5)(c_3^2 - c_1c_5 + c_2c_5^2 - c_3c_4c_5) > 0$

Table 1: Conditions for $P(\lambda)$ to have a pair of pure imaginary roots.

that define the locus of matrices that have eigenvalues whose sum is zero. They do not determine whether the roots are real or complex. For this purpose, one can use the theory of *subresultants* [49]. We observe that a common root of P and Q is imaginary if and only if the corresponding common root of \hat{R} and \hat{S} is negative. Therefore, we can give explicit inequalities in terms of the subresultants that determine whether a polynomial with a single, simple pair of roots whose sum is zero has a pair of pure imaginary roots. Table 1 gives a list of the equations and inequalities that determine the polynomials P of degree at most six with these properties.

The computation of characteristic polynomials of square matrices is computationally expensive and prone to numerical errors for some types of matrices. Thus, we seek methods that allow us to determine whether a matrix has a pair of pure imaginary eigenvalues without computing the characteristic polynomial as an intermediate step. This can be done through the definition of appropriate Kronecker or tensor products. The basic algebraic idea is that there are transformations of matrices that produce matrices whose eigenvalues are functions of the eigenvalues of the original matrix. For example, if A and B are square matrices, then the eigenvalues of the tensor product $A \otimes B$ are the pairwise products of the eigenvalues of A and those of B . If we form the transformation $T = I \otimes A + A \otimes I$ with I the $n \times n$ identity matrix, then the eigenvalues of T are sums of pairs of eigenvalues of A . To remove the redundancy associated with having both pairs $\lambda_i + \lambda_j$ and $\lambda_j + \lambda_i$ as eigenvalues, we use a skew-symmetric version construction. The *bialternate product* $A \odot I$ of A is the $n(n-1)/2 \times n(n-1)/2$ matrix defined by

$$(2\mathbf{A} \odot \mathbf{I}_n)_{\{pq,rs\}} = \begin{cases} -(A)_{p,s} & \text{if } r = q \\ (A)_{p,r} & \text{if } r \neq p \text{ and } s = q \\ (A)_{p,p} + (A)_{q,q} & \text{if } r = p \text{ and } s = q \\ (A)_{q,s} & \text{if } r = p \text{ and } s \neq q \\ -(A)_{q,r} & \text{if } s = p \\ 0 & \text{otherwise} \end{cases}$$

where the rows are labeled *lexicographically* by pq for $(p = 2, \dots, n; q = 1, \dots, p-1)$ and the columns likewise by rs for $(r = 2, \dots, n; s = 1, \dots, r-1)$ [23]. The eigenvalues of

$A \odot I$ are pairwise sums $\lambda_i + \lambda_j$ with $i < j$ of the eigenvalues of A . Thus, a necessary condition for A to have a pair of pure imaginary eigenvalues is that $A \odot I$ be singular. This singularity can be tested by computing the determinant of $A \odot I$, but we can also use other algorithms (such as singular value decomposition) from numerical linear algebra that give more accurate and robust tests for the singularity of A . In our ongoing work, we are implementing algorithms for tracking Hopf bifurcations based upon these algebraic methods and standard continuation methods.

4 Homoclinic Bifurcations and Their Computation

Bifurcation theory describes qualitative changes in phase portraits that occur as parameters are varied in the definition of a dynamical system. For dynamical systems defined by vector fields on R^n , one has a system of equations of the form $\dot{x} = f_\lambda(x)$ with $\lambda \in R^k$ denoting a k -dimensional vector of parameters. A rough classification of bifurcations distinguishes between *local* and *global* bifurcations, but it is difficult to make this distinction precise. Heuristically, the dynamics of local bifurcations are determined by information contained in the germ of the Taylor series of f or a Poincaré return map at a point, whereas the dynamics of global bifurcations require information about the vector field along an entire (non-periodic) trajectory. While the theory of bifurcations in multi-parameter families is far from complete, the theory of global bifurcations is more fragmentary than that of local bifurcations. A number of “codimension 2” global bifurcations have been studied, but there has not been an attempt to construct a synthesis of these studies that portrays a systematic view of the different cases and phenomena that occur. The lectures that were given in Montreal at this NATO sponsored summer school touched upon these matters, but these notes go much farther towards the construction of such a synthesis. We focus our attention on global bifurcations that involve homoclinic or heteroclinic orbits of equilibrium points of a vector field. We shall call homoclinic and heteroclinic orbits *connecting* orbits in order to have a common name for the two.

Silnikov seems to be the principal originator of the strategy we adopt to study global bifurcations with connecting orbits in higher dimensional vector fields. For planar vector fields, the techniques are older and asymptotic methods for studying global bifurcations in planar vector fields were well developed by the 1920’s (Dulac [15]). The fundamental idea is that the recurrent behavior near a connecting orbit should be studied in a fashion similar to that used in studying periodic orbits via a Poincaré return map. In particular, codimension one cross sections to the flow are introduced, and the return map of these cross sections is studied. There are some additional complications in the study of connecting orbits compared to that of periodic orbits which significantly complicate the analysis. We mention three of these. First, the discrete maps that describe flow past an equilibrium point are singular. In the simplest cases of flow past non-resonant equilibrium points, these “passage” or “correspondence” maps have singularities of the form x^a where a is not an integer and may be complex if the equilibrium has complex eigenvalues. These singularities lead to analysis that is much more complicated and intricate than that associated with the return map of a periodic orbit. As the work presented by Ilyashenko and Écalle at this summer school demonstrated, this analysis is frightfully complicated even for planar vector fields. The second complication arising from connecting orbits is that there are discontinu-

ities in the return maps of cross sections that are associated with connecting orbits. The bifurcations and attractors that appear in the Lorenz system [50] give a vivid example of the consequences of these discontinuities and have been described by Guckenheimer and Williams [37]. These discontinuities force one to look at dynamical systems that are built from multiple pieces rather than studying the iterates of a single continuous mapping. The third complication is that the list of cases of qualitatively different type is substantially longer than with local bifurcations. Tools for treating all of the cases in a single analysis are lacking, so the construction of a comprehensive and complete theory seems like a daunting task.

These lectures adopt a superficial view of the mathematical technicalities associated with global bifurcations. In constructing return maps for a flow along connecting orbits, one would like the simplest possible analytical expressions for these return maps. Normal form theory explores how coordinate changes can be used to simplify these analytical expressions, but the theory produces a large and intricate story whose details can mask many of the phenomena that we want to study. The idea of Šilnikov was to relax the requirement that an exact normal form be used to describe passage past an equilibrium and to use an approximation to the normal form instead. Asymptotic expansions for the flows and passage maps can be constructed, and one can begin the analysis of bifurcations with connecting orbits by using the leading term, or terms, of these asymptotic expansions. A similar approach to the global part of the flow producing returns to a cross section can also be used, but the asymptotic expansions of these smooth maps are given simply by Taylor series. A matching procedure can then be used to represent the full return map as a composition of singular and regular maps that come from passage past equilibrium and parts of the flow that are non-singular. In constructing maps with such matching procedures, we must remember that there may be discontinuities that lead to the examination of several different sequences of compositions. Following an analysis of return maps built from approximations, we can seek to determine the structural stability of the systems. It is unreasonable to expect that each type of bifurcation will have a structurally stable unfolding. We are plunged into the morass of considerations that result from the fact that structurally stable vector fields are not dense in the space of vector fields. The most that we try to do is to explore in each case which dynamical features of the bifurcation do persist under perturbations. Note that even specifying which perturbations are to be allowed in a theory based upon the return maps of connecting orbits is a tricky matter due to the singularities of the maps. Rather than engaging the reader in an extensive discussion of these problems, we proceed past them while erecting signposts that point in the direction of unresolved and incomplete technical matters.

4.1 Generic Homoclinic Orbits

Let $F : R^n \rightarrow R^n$ be a sufficiently smooth, vector field with a homoclinic orbit to an equilibrium point at 0. We shall denote the flow of F by ϕ_t and the homoclinic orbit by $\gamma(t)$. Let

$$\Gamma = \{\gamma(t) : t \in R\} \text{ where } \lim_{t \rightarrow \pm\infty} \gamma(t) = 0 \text{ and } \gamma(t) \neq 0.$$

We give a list of conditions that generic systems with a homoclinic orbit satisfy. These conditions help ensure that bifurcations from the homoclinic orbit have as simple a structure

as possible. In classifying codimension two bifurcations of homoclinic orbits, we can then look at events that cause the failure of one of these genericity conditions and examine the effect on bifurcations in two parameter families.

The first condition is that the equilibrium be hyperbolic and non-resonant. The non-resonance conditions that are important are primarily ones that involve the stable and unstable eigenvalues of smallest magnitude. We call these eigenvalues the *principal eigenvalues* of the equilibrium. More precisely, assume the linearization $D_x F(0)$ has k eigenvalues in the left half plane and $n - k$ in the right half plane. Assume there exists a real principal eigenvalue in the stable manifold denoted λ_s or a complex conjugate pair $\lambda_s, \bar{\lambda}_s$ with the property that if λ is another stable eigenvalue of $D_x F(0)$, then $\text{Re}(\lambda) < \text{Re}(\lambda_s) < 0$. Similarly, assume there exists a real principal eigenvalue in the unstable manifold denoted λ_u or a complex conjugate pair $\lambda_u, \bar{\lambda}_u$ with the property that if λ is another unstable eigenvalue of $D_x F(0)$, then $0 < \text{Re}(\lambda_u) < \text{Re}(\lambda)$.

At points in the stable and unstable manifolds of 0, there are filtrations of the tangent bundle associated with the exponential growth or decay of vectors as the trajectory approaches the origin. For a point p of the stable manifold, we are interested in three subspaces that we denote $E^{s+}(p) \supset E^s(p) \supset E^{ss}(p)$ and call the *stable plus weak unstable manifold*, the *stable manifold* and the *strong stable manifold*, respectively. These are defined via the variational equation for the trajectory through the point p given by

$$\dot{\xi} = (D_x F)|_{\phi_t(p)} \xi.$$

Let $V_t(v; p)$ denote the solution to this linear equation with initial condition $V_0(v; p) = v \in T_p R^n$. Let ν_s and ν_u be numbers such that

$$\text{Re}(\lambda) < \nu_s < \text{Re}(\lambda_s) < 0 \quad \text{or} \quad 0 < \text{Re}(\lambda_u) < \nu_u < \text{Re}(\lambda).$$

for any eigenvalue λ of $D_x F(0)$ which is not a principal eigenvalue. Then

$$\begin{aligned} E^{s+}(p) &\equiv \{v \in T_p R^n \mid \lim_{t \rightarrow +\infty} e^{-\nu_u t} |V_t(v; p)| = 0\} \\ E^s(p) &\equiv \{v \in T_p R^n \mid \lim_{t \rightarrow +\infty} |V_t(v; p)| = 0\} \\ E^{ss}(p) &\equiv \{v \in T_p R^n \mid \lim_{t \rightarrow +\infty} e^{-\nu_s t} |V_t(v; p)| = 0\}. \end{aligned}$$

There are analogous definitions of the *unstable plus weak stable manifold*, the *unstable manifold* and the *strong unstable manifold* of a point p in the unstable manifold of 0:

$$\begin{aligned} E^{u+}(p) &\equiv \{v \in T_p R^n \mid \lim_{t \rightarrow -\infty} e^{-\nu_s t} |V_t(v; p)| = 0\} \\ E^u(p) &\equiv \{v \in T_p R^n \mid \lim_{t \rightarrow -\infty} |V_t(v; p)| = 0\} \\ E^{uu}(p) &\equiv \{v \in T_p R^n \mid \lim_{t \rightarrow -\infty} e^{-\nu_u t} |V_t(v; p)| = 0\}. \end{aligned}$$

Note that there is no apparent relationship between these sets of manifolds at a point p of a homoclinic orbit other than that the vector field $F(p)$ belongs to both $E^s(p)$ and $E^u(p)$.

Our next requirement for a generic homoclinic orbit involves the direction of approach of a homoclinic orbit to 0 as $t \rightarrow \pm\infty$. Associated with the origin itself is a strong stable manifold W^{ss} consisting of points $p \in W^s$, the stable manifold of the origin as defined by the Stable Manifold Theorem, for which the vector field $F(p)$ lies in $E^{ss}(p)$. Note that $T_0 W^{ss} = E^{ss}(0)$ just as $T_0 W^s = E^s(0)$. Now W^{ss} is a proper submanifold of W^s of

codimension one or two depending upon whether the principal stable eigenvalue is real or complex. In either case, almost all trajectories in W^s lie in $W^s \setminus W^{ss}$. Similarly, almost all trajectories in W^u lie in $W^u \setminus W^{uu}$. Our next requirement for a generic homoclinic orbit is that a point p on Γ satisfy

$$p \notin W^{ss}, p \notin W^{uu}.$$

In words, (H3) is the statement that the homoclinic orbit approach the origin in the directions of the principal eigenvectors. This may alternatively be expressed by requiring that a point p on Γ satisfy

$$F(p) \notin E^{ss}, F(p) \notin E^{uu}.$$

The final condition that we impose upon generic homoclinic orbits involves the derivative of the flow along the homoclinic orbit. We state the condition in terms of the stable plus weak unstable and the unstable plus weak stable manifolds. Depending upon the types of the principal eigenvalues, the sum of the dimensions of $E^{s+}(p)$ and $E^{u+}(p)$ is $n+2$, $n+3$, or $n+4$. We require that the intersection $E^{s+}(p) \cap E^{u+}(p)$ be transverse and, furthermore, that $E^{s+}(p) \cap E^{uu}(p) = E^{ss}(p) \cap E^{u+}(p) = \{0\}$.

Let us examine the meaning of this final condition in the case of real eigenvalues. Assume that $\lambda_s, \lambda_u \in \mathbb{R}$. Then $\dim(E^{ss}) = m-1$ and $\dim(E^{uu}) = n-1$. Along Γ , the intersection $W^{s+} \cap W^{u+}$ is a two-dimensional bundle that contains the vector field. At the origin, this bundle approaches the plane spanned by the principal eigenvectors, both for $t \rightarrow +\infty$ and for $t \rightarrow -\infty$. We can think of this bundle as a “ribbon” along the homoclinic orbit that defines the behavior of the system in the “weak” directions that determine the primary structure of the orbit. Taking the closure at the origin of the bundle along the homoclinic orbit, we obtain a bundle of planes along a simple closed curve. This bundle is either orientable or non-orientable. We distinguish these cases by calling them *twisted* and *untwisted* homoclinic orbits. Twisted homoclinic orbits cannot occur for vector fields on orientable two-dimensional manifolds. Both twist types of homoclinic orbits are represented pictorially in Figure 3.

We will call a homoclinic orbit with real principal eigenvalues a *binodal* homoclinic orbit. For the generic binodal homoclinic orbit, there are no additional interesting dynamical structures in a sufficiently small neighborhood of the homoclinic orbit [62]. This is not necessarily true of generic homoclinic orbits with a complex principal eigenvalue. When exactly one of the principal eigenvalues is complex, we will call the homoclinic orbit a *unifocal* homoclinic orbit, and the generic case has been studied by Šilnikov [60, 62, 63] and others [24, 25, 29, 66]. The following two theorems describe the dynamical structures close to a generic unifocal homoclinic orbit, assuming that $\lambda_u \in \mathbb{R}$ and $\lambda_s \in \mathbb{C}$.

Theorem 4.1 *If $|\lambda_u/\operatorname{Re}(\lambda_s)| > 1$ (Šilnikov condition) then there exist horseshoes in every neighborhood of Γ .*

Theorem 4.2 *If $|\lambda_u/\operatorname{Re}(\lambda_s)| < 1$ then there is a neighborhood of Γ which contains no periodic orbits.*

The *non-resonance condition* on the principal eigenvalues is given by $|\lambda_u/\operatorname{Re}(\lambda_s)| \neq 1$. We may look at further conditions on the eigenvalues and determine a second genericity

requirement: $|\lambda_u/\text{Re}(\lambda_s)| \neq 2$. If $1 < |\lambda_u/\text{Re}(\lambda_s)| < 2$, then the linear flow at the origin is contracting and the horseshoes are attracting, while for $|\lambda_u/\text{Re}(\lambda_s)| > 2$ the linear flow at the origin is expanding.

Finally we consider the generic homoclinic orbit with complex principal eigenvalues which is called a *bifocal* homoclinic orbit. Figure 4 depicts the unifocal and bifocal homoclinic orbits. The bifocal homoclinic orbit has been studied by Šilnikov [61, 63], Glendinning [28], and Fowler and Sparrow [20]. They prove the following theorem:

Theorem 4.3 *There exist horseshoes in every neighborhood of a generic bifocal homoclinic orbit.*

4.2 Šilnikov Coordinates and Local Normal Forms

The unfoldings of the bifurcations involving connecting orbits can be very complicated. As we stated above, certain types of generic homoclinic orbits are embedded in much more complex dynamical structures. A full description of the unfolding of these orbits entails a comprehensive analysis of the horseshoes that are created or destroyed as a parameter is varied. These unfoldings have been studied for unifocal homoclinic orbits [24, 25, 29] and bifocal ones [20, 28]. We do not undertake such a monumentally complicated task, but we do want to describe maps that give an approximation to the return maps associated with homoclinic orbits. The general procedure we employ for doing this involves a decomposition of the return map for a homoclinic orbit into two parts: one describing the “local” part of the flow past the equilibrium point in the homoclinic orbit and the other describing the “global” portion of the flow outside of this neighborhood. In cases of singular cycles containing more than one connecting orbit, we make a decomposition into more pieces, but the principle is the same. In the decompositions that we use, we try to choose coordinates in a manner that simplifies the analytical expressions of the vector fields.

The simplest flows near an equilibrium point are linear. The question as to whether coordinate transformations near an equilibrium point can be found that linearize a vector field in a neighborhood of the equilibrium has been studied systematically for over a century, starting with Poincaré’s dissertation. The answers to the question are complicated. See Arnold [2] for an extensive summary of what is known about the linearization problem. Here we shall use a few bits of this theory. *Resonance conditions* on the eigenvalues provide the most elementary obstructions to linearization. A resonance condition of order k is expressed in terms of eigenvalues λ_j by $\lambda_i = \sum a_j \lambda_j$ with the a_j nonnegative integers whose sum is k . A vector field with an equilibrium point that satisfies a resonance condition of order k usually cannot be linearized by a C^k coordinate transformation. Nonetheless, there are *resonant normal forms* for the equilibrium with the property that there are smooth coordinate changes that transform the degree l Taylor series of the vector field at the equilibrium to its resonant normal form. We can hope in these situations that it is feasible to describe explicitly the flow of the resonant normal forms truncated to degree l and that these flows serve as good approximations to the flow of the original vector field in the vicinity of the equilibrium point. Here the classical theory breaks down and does not provide a good solution to the question as to when the passage map of two flows near an equilibrium are good approximations to one another.

Consider a *linear* vector field $\dot{x} = f(x)$ with a hyperbolic equilibrium point at the origin with k stable eigenvalues and $n - k$ unstable eigenvalues. Choose a coordinate system so that the stable and unstable manifolds W^s and W^u of the origin lie in coordinate planes. Let U_0 be a neighborhood of the origin that is the product of balls B_r^s and B_r^u of radius r in the stable and unstable manifolds W^s and W^u . The boundary of $B_r^s \times B_r^u$ is $\partial B_r^s \times B_r^u \cup B_r^s \times \partial B_r^u$. Since the vector field f is linear, the motion of points is the superposition of motions along the stable and unstable manifolds. Furthermore, the distance to the origin of points in the stable manifold decreases monotonically, while the distance to the origin of points in the unstable manifold increases monotonically, in a well chosen coordinate system. Therefore the passage map of U_0 will be defined as a map $\phi : \partial B_r^s \times B_r^u \rightarrow B_r^s \times \partial B_r^u$. With this choice of neighborhood of the origin, it is difficult to determine an explicit expression for the time of flight for a trajectory to reach the outgoing boundary of U_0 and hence to obtain a formula for ϕ . On the other hand, if we choose different neighborhoods of the origin, then we can sometimes compute the exit time from the neighborhood. In the case of real eigenvalues, we find that there are power law singularities; complex eigenvalues produce singularities with other elementary functions. Explicit examples are computed later.

For some problems of higher codimension, we shall need to compute the passage maps of equilibrium points that are either resonant or nonhyperbolic. In these cases, we shall still seek coordinate systems and approximations for which there are explicit integrals for the local normal forms at the equilibrium point. Cases with this property are the only ones considered in this paper, though there are higher codimension problems for which the normal forms are not integrable. In finding passage maps for these resonant cases, we would like to obtain formulas that remain valid when we perturb the equilibrium to make it generic. This requires some additional care beyond merely solving the explicit flows for the passage map at the resonant equilibrium.

The Šilnikov procedure is to combine the local passage maps near equilibria with nonsingular maps that describe the flow between cross sections around the portions of connecting orbits that do not contain equilibria. In the case of a homoclinic orbit, these cross sections can be taken to be portions of the boundary of the neighborhood U_0 that was used to construct the passage map past the equilibrium. As with the passage maps, we seek approximations for these “global” maps between cross sections. Since the maps are nonsingular, they can be approximated by truncating their Taylor series. Generally, we start with affine approximations to the transformations. If these are inadequate to obtain the (structural) stability results we seek, then higher degree approximations are used. The return map for a cross section can be obtained by composing these global maps with the local passage maps. In carrying through this composition, care must be taken with understanding the domains on which the maps are defined. When there are multiple connecting orbits, there is the additional possibility that flow in different directions away from an equilibrium may produce structures that require following different patterns of return to a neighborhood of the equilibrium.

4.3 Bifurcations From a Homoclinic Orbit: What Can We Study?

The difficulties of proving rigorous theorems about the unfoldings of bifurcations are formidable. Nonetheless, we would like to prove as much about phenomena that are consequences

of bifurcations of homoclinic and heteroclinic orbits as we can. Indeed, we would like to capture the major dynamical events that occur in the unfolding despite the fact that structural stability of the unfoldings will often fail. To make the theory “local” to the bifurcating orbits, we restrict attention to an arbitrarily small neighborhood of these orbits. Recurrent behavior that involves trajectories that leave such a neighborhood will be discussed separately. Here we describe three types of structures that can occur in small neighborhoods of bifurcating connecting orbits.

The first type of dynamical structure that can be involved at a homoclinic bifurcation is a periodic orbit. Generic bifurcations of binodal homoclinic orbits produce periodic orbits whose stability is determined by the sum of the principal eigenvalues at the saddle. In higher codimensions, multiple periodic orbits can bifurcate. In some cases (notably, the “gluing bifurcation” [45]), these orbits and their patterns of bifurcations can be complicated. The second type of dynamical structure produced in bifurcations of connecting orbits is typified by the homoclinic bifurcation in the Lorenz system [50]. In this system, for reasons of symmetry, a pair of homoclinic orbits are formed. As they bifurcate, a horseshoe is immediately created. The same phenomenon occurs in higher codimension bifurcations without symmetry. Third, generic homoclinic orbits with complex values may be adjacent to horseshoes. As described by Šilnikov [60], homoclinic orbits to equilibria satisfying appropriate conditions on their eigenvalues occur only in the closure of horseshoes. As the homoclinic orbit is unfolded, the horseshoes closest to the homoclinic orbit can be destroyed.

The singularity theory for mappings between two spaces is much “cleaner” than the bifurcation theory of flows (or iterated mappings). There are a number of reasons for these differences, one being the complex dynamical structures that occur in unfoldings of certain bifurcations. If there are horseshoes that are created or destroyed as part of a bifurcation, then the unfolding of these bifurcations will involve all of the associated complications. These have been studied most thoroughly in the context of the Hénon mapping [6, 52]. There are an infinite number of bifurcations of periodic orbits that are part of the creation of horseshoes. If there is a single unstable eigenvalue and volume contraction in these flows, there are also phenomena such as infinitely many (Newhouse) sinks and the occurrence of nonhyperbolic strange attractors [36]. We do not want to become enmeshed in these details. To a large extent they appear to be subsidiary to the fact that horseshoes are created, and we expect to add little to the general discussion of the processes associated with the creation and destruction of the horseshoes. Our focus in dealing with horseshoes will be to demonstrate that a return map in an unfolding satisfies the conditions that guarantee the existence of horseshoes. We will not generally explore whether the horseshoe is part of a larger invariant set or investigate the presence of nonhyperbolic invariant sets in the unfoldings.

4.4 Codimension Two Bifurcations of Connecting Orbits

There are many types of codimension two bifurcations of connecting orbits. Failure of one of the conditions that characterize a generic homoclinic orbit will lead to a degenerate bifurcation. These can be classified into four groups:

1. Eigenvalue degeneracies

2. Degenerate approach
3. Degenerate twist
4. Multiple connecting orbits

Each of these types can be further subdivided. For example, the eigenvalue degeneracies may be due to a single zero eigenvalue, a pair of pure imaginary eigenvalues, equal magnitude of the real parts of the principal eigenvalues, or equal magnitude of a real principal eigenvalue with the sum of a pair of imaginary principal eigenvalues. Furthermore, one has a different analysis depending on whether the homoclinic orbit is nodal, unifocal or bifocal, and, in the nodal case, the twist associated with a resonance. In all of the cases that have been studied, the introduction of Šilnikov coordinates and the study of return maps built from these coordinates is a major portion of the analysis of the bifurcation. Rigorous results that go beyond the description of model systems tend to be very difficult to formulate and prove. When there are horseshoes associated with these bifurcations, even the phenomenology associated with the Šilnikov approximations tends to be incomplete.

Below we discuss a bifurcation with an eigenvalue degeneracy, one with a degenerate approach, and another with multiple connecting orbits, describing each in terms of Šilnikov approximations. Additionally, within each category, we give a survey of other work known to us. For the case of degenerate approach, we refer the reader to the work of Terman [65].

4.5 Eigenvalue Degeneracies

There are a number of different eigenvalue degeneracies which may occur. Non-hyperbolic equilibrium point degeneracies have been studied by, in the nodal case, Deng [12], Luk'yanov [51] and Schecter [56]; in the case of unifocal homoclinic orbits with a nonhyperbolic saddle, Belyakov [5]; and, in the case of unifocal homoclinic orbits with a nonhyperbolic focus, Argoul, Arneodo and Richetti [1, 54], Bosch and Simo [8], Gaspard and Wang [26], and Hirschberg and Knobloch [41]. Here we will look at vector fields that have a homoclinic orbit with real principal eigenvalues of equal magnitude. The homoclinic orbit may be twisted or untwisted, and the bifurcation is different, depending on the case. This has been studied by a number of different authors, including Glendinning [27], Kokubu [47], and Chow, Deng, and Fiedler [9].

A normal form for a planar saddle with a 1:1 resonance is given by the system

$$\begin{aligned}\dot{x} &= -x(1 + xy) \\ \dot{y} &= y\end{aligned}$$

An unfolding of this system allows the ratio of eigenvalues at the origin to vary:

$$\begin{aligned}\dot{x} &= -x(1 + \lambda + xy) \\ \dot{y} &= y\end{aligned}$$

To use Šilnikov coordinates for these systems we seek to integrate the normal form explicitly and solve for the passage map past the origin. The trajectory with initial conditions (x_0, y_0)

is

$$\begin{aligned} x(t) &= \frac{e^{-(1+\lambda)t}}{\frac{1}{x_0} + \frac{y_0}{\lambda}(1 - e^{-\lambda t})} \\ y(t) &= y_0 e^t \end{aligned}$$

and the passage map from the line $x = 1$ to the line $y = 1$ has a time of flight $t = -\ln(y)$ and an expression

$$x = \psi(y) = \frac{y^{(1+\lambda)}}{1 + \frac{y}{\lambda}(1 - y^\lambda)} . \quad (1)$$

When $\lambda \rightarrow 0$, this map becomes

$$x = \psi(y) = \frac{y}{1 - y \ln y} .$$

The leading order term in Equation 1 is $y^{(1+\lambda)}$ and is adequate for the calculation of the unfolding of the codimension two bifurcations of the homoclinic orbit. The global portion of the Šilnikov approximation to the return map is an affine transformation $y = ax + \mu$. We assume that $a \neq \pm 1$ and that μ is the second parameter of the unfolding. Thus the approximate return map is $\phi(y) = ay^{(1+\lambda)} + \mu$.

If the homoclinic orbit is untwisted, then $a > 0$. If the homoclinic orbit is twisted, then $a < 0$. The domain of ϕ is a segment with endpoint at $y = 0$. We analyze ϕ first in the untwisted case. There is a periodic orbit close to the homoclinic orbit if ϕ has a fixed point. The periodic orbit is degenerate if its fixed point p satisfies $\phi'(p) = 1$. This happens when $\mu = p - ap^{(1+\lambda)}$ and $a(1 + \lambda)p^\lambda = 1$. If we eliminate p from this pair of equations, we obtain

$$\mu = \lambda(1 + \lambda)^{-(1+1/\lambda)} a^{-1/\lambda} .$$

As $\lambda \rightarrow 0$, this gives $\mu \approx \lambda e^{-1} a^{-1/\lambda}$. In order that μ be small, we need to choose the sign of λ so that $\lambda \ln a > 0$. Thus λ is positive if $a > 1$ and λ is negative if $0 < a < 1$. Observe that the curve in the (λ, μ) plane along which nonhyperbolic periodic orbits occur has a flat tangency with the curve $\mu = 0$ along which there are homoclinic orbits. In the thin wedge between the two, there are two periodic orbits near the location of the degenerate homoclinic orbit. See Figure 5.

The analysis of the twisted case is similar, but there is indeed a new twist. The return map has the form described above, but $a < 0$. This makes the return map ϕ a decreasing function of y . As a result, there are two kinds of periodic orbits and two kinds of homoclinic orbits in the unfolding: “once rounding” and “twice rounding”. The once rounding loops are twisted while the twice rounding loops are untwisted. The once rounding periodic orbits have a negative principal characteristic multiplier while the twice rounding orbits have a positive multiplier. The transition between the two is given by a period doubling bifurcation. Thus there are three different types of bifurcations that occur in the unfolding of the twisted resonant loop: once rounding homoclinic orbits, twice rounding homoclinic orbits and period doubling bifurcations of periodic orbits. These can be computed in terms of the return map $\phi(y) = ay^{(1+\lambda)} + \mu$. The once rounding homoclinic orbits are given by $\mu = 0$. The twice rounding homoclinic orbits are given by parameters for which $0 =$

$\phi^2(0) = \phi(\mu) = a\mu^{(1+\lambda)} + \mu$. Solving this equation for μ yields $\mu = |a|^{-1/\lambda}$. The period doubling bifurcations occur at fixed points of ϕ for which the return map has derivative -1 : $a(1+\lambda)p^\lambda = -1$ and $\mu = p - ap^{(1+\lambda)}$. This yields

$$\mu = \left(\frac{2+\lambda}{1+\lambda}\right)(1+\lambda)^{-1/\lambda}|a|^{-1/\lambda}.$$

As $\lambda \rightarrow 0$, observe that the ratio of the values of μ that produce period doubling and twice rounding homoclinic orbits approaches $2/e$. This ratio is a “universal” property of this codimension two bifurcation. As with the untwisted resonant bifurcation, the bifurcation curves have a flat tangency. See Figure 6.

4.6 Inclination Degeneracies

When the principal eigenvalues of a homoclinic orbit are real, but the homoclinic orbit is neither twisted nor untwisted, then there is an inclination degeneracy. This situation has been studied by Deng [14], and there are many subcases that lead to different bifurcation diagrams. Here we describe one of these cases, illustrating that horseshoes can occur in the unfolding of this codimension two global bifurcation. The example also illustrates a circumstance in which an approximate return map that comes from the composition of an affine map with a local passage transformation does not capture all of the important dynamical behavior.

Three is the lowest dimension in which one can construct a homoclinic orbit with degenerate twist. We consider a two parameter family of vector fields that are linear in a neighborhood of the origin, with two real stable eigenvalues $\lambda_y < \lambda_x < 0$ and an unstable real eigenvalue $\lambda_z > 0$. We assume that there is a homoclinic orbit that approaches the origin along the x axis in forward time and along the z axis in backward time. We shall assume further that the return map for the orbit is degenerate in the twisting of the normal bundle around the homoclinic orbit. This means that a vector, pointing in the direction of the principal stable eigenvector as the homoclinic orbit leaves the origin, returns in the direction of the strong stable manifold (rather than the generic behavior of returning in the direction of the unstable manifold).

Let us view the situation in terms of a Šilnikov approximation. The passage map near the origin from the cross section Σ defined by $x = 1$ to the cross section $z = 1$ will be given by

$$\begin{pmatrix} u \\ v \end{pmatrix} = \psi \begin{pmatrix} y \\ z \end{pmatrix} = \begin{pmatrix} z^\alpha \\ yz^\beta \end{pmatrix}$$

where

$$\alpha = -\lambda_x/\lambda_z, \beta = -\lambda_y/\lambda_z, 0 < \alpha < \beta.$$

Here and below, if $z < 0$, we denote $z^\alpha = -(-z)^\alpha$. The global return from $z = 1$ to $x = 1$ will be approximated by

$$\begin{pmatrix} y \\ z \end{pmatrix} = \gamma \begin{pmatrix} u \\ v \end{pmatrix} = \begin{pmatrix} c \\ \lambda \end{pmatrix} + \begin{pmatrix} au + bv \\ -\mu u + u^2 + v \end{pmatrix}.$$

Then the return map ϕ is approximated by

$$\phi \begin{pmatrix} y \\ z \end{pmatrix} = \begin{pmatrix} c + az^\alpha + byz^\beta \\ \lambda - \mu z^\alpha + z^{2\alpha} + yz^\beta \end{pmatrix}.$$

Here the parameter λ determines whether a homoclinic connection occurs, while the sign of μ determines whether the connection is twisted or untwisted. Note that the approximation has included a quadratic term in γ . Without this term, the plane spanned by the principal eigenvectors would return entirely within the stable manifold, a highly degenerate situation.

There are now several cases determined by the relative magnitude of the exponents α and β . The case we shall examine is the one in which we assume that $2\alpha < \beta$ and $\alpha < 1/2$. The first of these assumptions implies that $|yz^\beta| = o(z^{2\alpha})$ and the second leads to complex dynamical behavior involving the stretching in the z direction. We shall not try to give a complete analysis of even the specific family of maps defined by ϕ , but we shall show that there are horseshoes that appear in some regions of the parameter space for this family.

The assumption $2\alpha < \beta$ leads to an approximation of ϕ by a one-dimensional mapping. The nature of the approximation will be examined below. Consider the one-dimensional mapping $\hat{\phi}(z) = \lambda - \mu z^\alpha + z^{2\alpha}$ obtained by ignoring the y coordinate in the definition of ϕ . This is a unimodal map, and we look for ranges of parameter values for which this mapping will have a hyperbolic invariant set. If $\lambda = 3\mu^2/16$ and $\mu > 0$, $\hat{\phi}(z) = (z^\alpha - \mu/4)(z^\alpha - 3\mu/4)$. Let

$$A = 0, \quad B = (\mu/4)^{1/\alpha}, \quad C = (3\mu/4)^{1/\alpha}, \quad D = \mu^{1/\alpha},$$

so $A < B < C < D$. Then $\hat{\phi}(A) = \hat{\phi}(D) = 3\mu^2/16 \gg D$ since $\alpha < 1/2$, and $\hat{\phi}(B) = \hat{\phi}(C) = A$. Now $|\hat{\phi}'(B)| = |\hat{\phi}'(C)| = 2\alpha(-\mu/4)^{2-1/\alpha} > 1$ for $-\mu$ small. Since $\hat{\phi}([A, B]) \supset [A, D]$, $\hat{\phi}([C, D]) \supset [A, D]$, and $\hat{\phi} > 1$ on $[A, B]$ and $[C, D]$, we conclude that the map $\hat{\phi}$ has a hyperbolic invariant set in the interval $[A, D) = [0, \mu^{1/\alpha})$.

In the cross section Σ , consider the rectangle $R_\mu = [c - 2\mu^{1/\alpha}, c + 2\mu^{1/\alpha}] \times [-2\mu^{1/\alpha}, 2\mu^{1/\alpha}]$. If we set $\lambda = 3\mu^2/16$ and let $\mu \rightarrow 0$ from below, then the return maps of the rectangles R_μ can be rescaled so that they tend to a map of rank 1. The rescaled maps have a vertical coordinate that behaves as a rescaled version of $\hat{\phi}$. This situation is analogous to the behavior of the Hénon map [40] in the limit as the map tends to a map of rank one. The hyperbolic invariant set will persist as a horseshoe as we leave the singular limit $\mu \rightarrow 0$. The analysis of Benedicks and Carleson [6], extended by Mora and Viana [52] indicates further that as λ varies, we will expect to encounter chaotic attractors for the return map ϕ .

4.7 Multiple Connections

Consider a vector field in a generic two-parameter family that has an equilibrium point with a single unstable eigenvalue, real non-resonant principal eigenvalues and a pair of generic homoclinic orbits formed from the two unstable separatrices of the saddle point. We would like to analyze the unfoldings of such systems. In the planar case, this determines the geometry of the unfolding of the family and is described below. On the other hand, there are several choices that occur if the vector field has dimension at least three. In particular, if the two homoclinic orbits approach the equilibrium from the same direction along the principal stable eigenvector, then there are cases that lead to either geometric Lorenz attractors [37]

or to complex periodic orbits formed by the *gluing bifurcations* described by Gambaudo, Glendinning and Tresser [45]. We recall bits of their analysis below.

Let X be a planar vector field with a non-resonant hyperbolic equilibrium point at the origin and a pair of orbits homoclinic to the origin. Assume that X is contained in a generic two parameter family of vector fields. There are two topologically distinct configurations depending upon whether one homoclinic orbit is contained in the other, but there is little difference in the analysis of the two cases. Pick a pair of cross sections Σ_1, Σ_2 to the two stable separatrices and consider the return map $\phi : \Sigma_1 \cup \Sigma_2 \rightarrow \Sigma_1 \cup \Sigma_2$. This return map will have discontinuities at the intersections of Σ_1 and Σ_2 with the stable manifold of 0. Thus we can think of ϕ as constructed from four maps $\phi_{ij} : \Sigma_i \rightarrow \Sigma_j$. These maps fit together so that the ranges of ϕ_{1j} and ϕ_{2j} are contiguous and do not overlap. At the common endpoint of the images, there is a singularity of the form x^α with $\alpha \neq 1$. By reversing time if necessary, we may assume that the magnitude of the stable eigenvalue of 0 is larger than the unstable eigenvalue, implying $\alpha > 1$ and that the derivatives of the ϕ_{ij} are smaller than 1 near the stable manifold of 0. Furthermore, we may choose orientations of Σ_1 and Σ_2 so that the maps ϕ_{ij} are increasing. Then each ϕ_{ij} or iterates of the ϕ_{ij} in a connected domain can have at most one fixed point, and that point will be stable. Determining which types of periodic orbits bifurcate from the double loop becomes a matter of determining which configurations of fixed points for iterates of the maps ϕ_{ij} can occur. The cross sections and return maps are pictured in Figure 7.

Denote once again $x^\alpha = -(-x)^\alpha$ for $x < 0$ and choose coordinates on cross sections that are centered on the stable manifolds. The Šilnikov approximation for the return maps have the form $\phi_{ij}(x) = a_j x^\alpha + b_j$, but one must remember that there are two components to the domain of the return map and ϕ_{12} and ϕ_{21} map one domain to the other. Here b_1 and b_2 can be regarded as the unfolding parameters of the system.

It is important here that the maps ϕ_{1j} and ϕ_{2j} have contiguous images. There are three kinds of periodic orbits for the return maps that correspond to periodic orbits of the flow: fixed points of ϕ_{ii} and fixed points of a composition $\phi_{12} \circ \phi_{21}$ or $\phi_{21} \circ \phi_{12}$. The fixed points of ϕ_{ii} correspond to periodic orbits that lie close to one of the homoclinic orbits, while the fixed points of $\phi_{12} \circ \phi_{21}$ and $\phi_{21} \circ \phi_{12}$ correspond to periodic orbits that lie close to both of the homoclinic orbits from the system. All of the periodic orbits in a neighborhood of the double homoclinic orbit have a stability that is determined by whether the Jacobian of the non-resonant saddle at the origin has a positive trace (unstable) or negative trace (stable). The boundaries between the parameter regions with different types of periodic orbits will be given by parameter values at which homoclinic orbits occur. There are four types of homoclinic orbits. In terms of the return map these correspond to fixed points at 0 of ϕ_{11} , ϕ_{22} , $\phi_{12} \circ \phi_{21}$ and $\phi_{21} \circ \phi_{12}$. The parameter curves yielding the first two types of homoclinic orbits are simply $b_1 = 0$ and $b_2 = 0$. The parameter values yielding the more complicated homoclinic orbits are given by $a_2 b_1^\alpha + b_2 = 0$ and $a_1 b_2^\alpha + b_1 = 0$. Since the return maps are orientation preserving, $a > 0$, and taking the domain and ranges into account, these curves of bifurcating homoclinic orbits occur in the quadrants of the (b_1, b_2) plane in which b_1 and b_2 have opposite signs. This completes the description of the unfolding of this codimension two bifurcation.

In higher dimensions, double homoclinic orbits can be more complicated than the ones that occur for planar vector fields. The additional complication is due to the fact that

the return maps along two separatrices of a one-dimensional unstable manifold need not match in the same fashion that they do for a planar vector field. If the unstable eigenvalue is smaller in magnitude than all of the stable eigenvalues, then the periodic orbits that bifurcate from the homoclinic cycles are all stable, and there are only a finite number of them for any given parameter value. Indeed there are at most two. The situation that we describe was analyzed by Gambaudo, Glendinning and Tresser [45], who called this the *gluing bifurcation*. Their analysis is based upon the study of return maps for the double cycle. Let us describe a bit more.

Let X be a vector field on R^n with an equilibrium point at the origin having a single unstable eigenvalue λ_u and a stable eigenspace of dimension $n-1$ whose spectrum lies to the left of the line $Re(\lambda) < -\lambda_u$. Assume further that both unstable separatrices of the origin are homoclinic, and that X is embedded in a generic two parameter family. Form a cross section Σ to the stable manifold $W^s(0)$ near the origin and let the components of $\Sigma - W^s(0)$ be Σ_1 and Σ_2 . The return maps ϕ_1 and ϕ_2 of Σ_1 and Σ_2 will be continuous, contracting and have images that are punctured neighborhoods of the (first) intersection of each unstable separatrix with Σ . Thus we can abstract the situation that we encounter to the study of the “quasicontractions” $\phi_1 : \Sigma_1 \rightarrow \Sigma$ and $\phi_2 : \Sigma_2 \rightarrow \Sigma$. If the images of these maps intersect $W^s(0)$, then there will be more components formed from subsequent compositions of ϕ_1 and ϕ_2 . Using “symbolic dynamics”, one can analyze the periodic orbits that can form from the iterated compositions of a pair of maps. The following one-dimensional model is adequate to represent the general situation. Consider a map $f : [-1, 1] \rightarrow [-1, 1]$ that is discontinuous at the origin and contracting. The “kneading theory” or symbolic dynamics of f characterize its behavior. This gives a combinatorial procedure for determining the dynamics of f from the trajectories of the points $-1, 0^-, 0^+, 1$. For maps of the form of f , there are zero, one or two periodic orbits. The patterns of signs of $f^i(x)$ along periodic orbits are greatly restricted and can be assigned a *signature* that is a rational number. When there are two periodic orbits, their signatures $p/q, p'/q'$ are *Farey neighbors*; i.e., $|pq' - qp'| = 1$. The different families of periodic orbits appear and disappear in complex homoclinic orbits. Thus, even without the occurrence of horseshoes, the gluing bifurcation has an unfolding with an infinite number of curves in its bifurcation set.

Other connecting orbit bifurcations have been studied by Chow, Deng and Fiedler [10], Deng [13], Glendinning and Sparrow [30], Glendinning and Tresser [31], and Schechter [57, 58]

4.8 Computations of Connecting Orbits

The numerical computation of connecting orbits has only recently been investigated, and the construction of robust algorithms that effectively compute connecting orbits in large classes of vector fields remains a challenge. We make a few comments concerning the numerical difficulties and fewer suggestions for how these difficulties might be confronted. We seek to solve the following problems. In generic one parameter families of vector fields, there are isolated points with connecting orbits between equilibrium points. We want accurate calculations of these parameter values and of the resulting orbits. (There may also be accumulation points of connecting orbits of increasing length and complicated topological structure in generic one parameter families [4].) In generic two parameter families of vector fields, there are curves of parameter values at which connecting orbits occur. We seek to use

continuation methods to compute these curves. The endpoints of these curves of homoclinic and heteroclinic bifurcations are frequently global codimension two bifurcations. We seek to classify these codimension two bifurcations and construct algorithms for their computation. The unfoldings of some of these codimension two bifurcations have been described above, but there is a long list of cases that have yet to be analyzed fully – even at the level of Šilnikov approximations. Thus the goal of implementing the computation of unfoldings of global codimension two bifurcations involves mathematical as well as computational questions.

Generic connecting orbits are intersections of stable and unstable manifolds of equilibria. Therefore, algorithms for the reliable calculation of these invariant manifolds might seem to form the basis for computation of the connecting orbits. This strategy is clearly an expensive one from a computational point of view, so we seek more direct methods for computing connecting orbits. In practice, most examples in higher dimensional vector fields have been computed by tracking periodic orbits that bifurcate from homoclinic orbits, with high period periodic orbits used as approximations to the homoclinic orbits. When the periodic orbits involved are not stable, then tracking the periodic orbits requires the use of algorithms for solving boundary value problems or algorithms that find fixed points of a cross section. Since the periodic orbits usually disappear at the homoclinic orbit, these computations are hard to implement in an automatic fashion. We seek methods that are more direct.

Mathematically, a connecting orbit is the solution of a boundary value problem on an infinite interval of time. To construct algorithms based upon boundary value solvers for finding connecting orbits, one wants to convert the problem into one involving a finite time interval. This can be done approximately by introducing linear (or polynomial) approximations for the local stable and unstable manifolds containing the ends of the connecting orbits and seeking trajectories that begin on the local unstable manifold and end on the local stable manifold. Beyn [7], Chow and Lin [11], Doedel and Friedman [21, 22] and Schecter [59] have all considered algorithmic aspects of the computation of homoclinic orbits, but the only computations that have been examined carefully involve planar vector fields.

One of the pragmatic questions concerning the computation of homoclinic bifurcations is whether the goal is to obtain an accurate approximation of the parameter values at which the bifurcation occurs or whether one is primarily interested in the computation of an accurate approximation to the homoclinic orbit. These are substantially different questions for reasons that we now describe. Suppose a small error has been made in the determination of the parameter value μ for which there is a homoclinic orbit in a system. We ask whether there is a trajectory for parameter value μ' that closely approximates the homoclinic orbit that exists for parameter value μ . The distance of closest approach between the stable and unstable manifolds will be of order $\mu - \mu'$ since compact portions of the manifolds vary smoothly with the parameters. Thus we want to know how close the trajectory through a point close to the stable manifold comes to the equilibrium. Estimates can be obtained from linear vector fields.

Consider a linear vector field X with a hyperbolic equilibrium point at the origin and assume that the stable and unstable manifolds are coordinate subspaces. The vector field “separates” into a stable system and an unstable system. Along trajectories, the unstable coordinates grow at an exponential rate. Now look at a generic point x on the stable manifold and estimate the distance of closest approach to the equilibrium point of a trajectory

passing through a point x' close to x . If the difference $x' - x$ has a non-zero component in the direction of the strongest unstable eigenvalue of X , then this component will grow exponentially at a rate which is the eigenvalue of the strongest unstable eigenvalue. As we saw above, a generic point on the stable manifold approaches the equilibrium in the direction of the principal (weakest) stable eigenvalue. Putting these observations together, we estimate the point of closest approach to the origin of the trajectory through x' as having order c^β where c is the component of x' in the strongest unstable direction and β is the ratio of the magnitude of the principal stable eigenvalue to the strongest unstable eigenvalue. When $1/\beta$ is large, then small errors in locating a point on the unstable eigenvalue lead to much larger distances between the closest trajectory and the homoclinic orbit that is sought. If we formulate a boundary value problem to find the homoclinic orbit, then we will need to start with a very good approximation to the homoclinic orbit to have hope of being able to use the boundary value solver. Trajectories depend very sensitively upon the parameters in a neighborhood of the equilibrium. These difficulties become still more extreme if one seeks the computation of a unifocal homoclinic orbit.

We have attempted to point out some of the difficulties associated with the computation of connecting orbits. The computation of these dynamical structures is important due to their role in organizing the dynamics of a system. Consequently, this is an interesting problem.

5 An Example: The Hodgkin and Huxley Equations

This section describes the analysis of a moderately complicated dynamical system and is work done in collaboration with Isabel Labouriau. The Hodgkin and Huxley (HH) equations are a “simple” neuron model developed from experiments performed with a squid [43]. These equations relate the difference of electric potential across the cell membrane (V) and gating variables (m , n , and h) for ion channels, to the stimulus intensity (I), and temperature (T), as follows:

$$\begin{cases} \dot{V} &= -G(V, m, n, h) + I \\ \dot{m} &= \Phi(T) [(1 - m)\alpha_m(V) - m\beta_m(V)] \\ \dot{n} &= \Phi(T) [(1 - n)\alpha_n(V) - n\beta_n(V)] \\ \dot{h} &= \Phi(T) [(1 - h)\alpha_h(V) - h\beta_h(V)] \end{cases} \quad (\text{HH})$$

where \dot{x} stands for dx/dt and Φ is given by $\Phi(T) = 3^{(T-6.3)/10}$. The other functions involved are:

$$G(V, m, n, h) = \bar{g}_{\text{Na}} m^3 h (V - \bar{V}_{\text{Na}}) + \bar{g}_{\text{K}} n^4 (V - \bar{V}_{\text{K}}) + \bar{g}_{\text{L}} (V - \bar{V}_{\text{L}})$$

and the equations modeling the variation of membrane permeability:

$$\begin{aligned} \alpha_m(V) &= \Psi\left(\frac{V+25}{10}\right) & \beta_m(V) &= 4e^{V/18} \\ \alpha_n(V) &= 0.1\Psi\left(\frac{V+10}{10}\right) & \beta_n(V) &= 0.125e^{V/80} \\ \alpha_h(V) &= 0.07e^{V/20} & \beta_h(V) &= \left(1 + e^{(V+30)/10}\right)^{-1} \end{aligned}$$

$$\text{with} \quad \Psi(x) = \begin{cases} x/(e^x - 1) & \text{if } x \neq 0 \\ 1 & \text{if } x = 0 \end{cases}.$$

Notice that $\alpha_y(V) + \beta_y(V) \neq 0$ for all V and for $y = m, n$ or h . The parameters $\bar{g}_{\text{ion}}, \bar{V}_{\text{ion}}$ representing maximum conductance and equilibrium potential for the ion were obtained from experimental data by Hodgkin and Huxley, with the values given below:

$$\begin{array}{lll} \bar{g}_{\text{Na}} = 120 \text{ mS/cm}^2 & \bar{g}_{\text{K}} = 36 \text{ mS/cm}^2 & \bar{g}_{\text{L}} = 0.3 \text{ mS/cm}^2 \\ \bar{V}_{\text{Na}} = -115 \text{ mV} & \bar{V}_{\text{K}} = 12 \text{ mV} & \bar{V}_{\text{L}} = 10.599 \text{ mV} \end{array}$$

The values \bar{V}_{Na} and \bar{V}_{K} can be controlled experimentally [42]. For the results in this paper, we use the temperature $T = 6.3^\circ\text{C}$ and, except where stated explicitly, all the other parameters involved in the HH equations have the values quoted above that we call the HH values.

We describe some of the bifurcations of the HH equations as an illustration of the theory and algorithms described above. The local bifurcations of equilibria were calculated in terms of the the derivatives of the HH equations at the equilibrium points. Global bifurcations could only be studied by numerically integrating the HH equations. Our analysis of local bifurcations used the symbolic computer program Maple to implement the calculation of saddle-node and Hopf bifurcation curves. For $y = m, n$, or h the equation for \dot{y} in (HH) is linear in y , so the last three components of an equilibrium solution (V_*, M_*, N_*, H_*) of (HH) can be written as functions of V_* :

$$y_* = y_\infty(V_*) = \frac{\alpha_y(V_*)}{\alpha_y(V_*) + \beta_y(V_*)} \quad \text{for } y = m, n, h .$$

Substituting y_* for $y = m, n, h$ in the first equation, we get:

$$G(V_*, m_\infty(V_*), n_\infty(V_*), h_\infty(V_*)) = f(V_*) = I .$$

Thus, for fixed \bar{V}_{K} there is exactly one value of I for which (V_*, m_*, n_*, h_*) is at equilibrium. Note that derivatives of (HH) are independent of I .

When \bar{V}_{K} has the HH value of 12 mV, f is monotonic and (HH) has a unique equilibrium for each value of I . For fixed lower values of \bar{V}_{K} , there are two saddle-node bifurcations as I is varied, creating a region with three equilibria. The two curves of saddle-nodes terminate at a cusp point. See also [44]. The saddle-node curves in the $I \times \bar{V}_{\text{K}}$ plane were computed parametrically with V_* as the independent parameter. The equations describing the saddle-node curves involve the determinant of the matrix of first derivatives of (HH) at an equilibrium point. We calculated an explicit expression for this determinant symbolically with Maple. By solving the equation that the determinant vanishes for \bar{V}_{K} at equilibrium values of (V_*, m_*, n_*, h_*) , we obtained the curve $\bar{V}_{\text{K}}(V_*)$ of parameter values corresponding to zero eigenvalues.

To determine the parameter values at which Hopf bifurcation occurs, it is necessary to compute eigenvalues of the matrix of first derivatives of (HH) at an equilibrium point. There is a pair of purely imaginary eigenvalue when the characteristic polynomial $x^4 + c_3x^3 + c_2x^2 + c_1x + c_0$ of this matrix satisfies simultaneously the third degree equation $c_1^2 - c_1c_2c_3 + c_0c_3^2 = 0$ and the inequality $c_1c_3 > 0$. These are the expressions that result from the Sylvester resultant calculation described earlier. Again, we computed this equation symbolically, assuming a given value of V_* , and solved for \bar{V}_{K} . The graph we obtained for the solution of this equation and inequality disagrees slightly with the findings of Holden, *et*

al., [44] for the HH value $\bar{g}_K = 36$. Takens-Bogdanov bifurcations occur when the equations defining Hopf bifurcations and saddle-node bifurcations are satisfied simultaneously.

The saddle-node and Hopf bifurcations are the only codimension one bifurcations that can be computed explicitly from (HH) without numerical integration. The presence of double cycles where the two periodic orbits created at Hopf bifurcation points coalesce and disappear has been established previously [39, 48, 55] and the existence of saddle loops emanating from the Takens-Bogdanov points is predicted by bifurcation theory [36]. To determine further information about global bifurcations, we rely upon numerical integrations that were performed with the computer program *DsTool* [3]. This program establishes a graphical interface and display for investigating bifurcations of dynamical systems. It allows one to mark points in a two-dimensional parameter space with identifying symbols and to display phase portraits that correspond to these points. The computed data for local bifurcations was displayed in the parameter space window. By searching for the boundaries of parameter regions yielding structurally stable dynamics and using our knowledge of the unfoldings of codimension two bifurcations, we deduced the location of curves along which global bifurcations take place. We obtain a consistent picture of the bifurcation diagrams for (HH) in the two-dimensional $I \times \bar{V}_K$ parameter plane. These diagrams have not been proved to be correct, but they are based upon strong numerical evidence.

The bifurcation diagram resulting from our numerical investigations is shown in Figure 8.

Its main features include a curve of double cycles (dc) which enters the cusp region with three equilibrium points and terminates at a degenerate Hopf bifurcation (dh) close to the Takens-Bogdanov point (tb). These double cycles are the ones described in [48]. The curve of saddle loops (sl) emanating from the Takens-Bogdanov point crosses the Hopf curve beyond the degenerate Hopf point, and then turns sharply. From this sharp bend, it proceeds almost parallel to the saddle-node curve (sn). The saddle loops appear to undergo a reversal of orientation along this portion of the curve (sl). After the orientation has reversed, one encounters a set of parameters at which the unstable eigenvalue and the weakest stable eigenvalue have equal magnitudes. This point (tsl) in parameter space is a twisted neutral saddle loop, and there are additional curves of untwisted twice rounding and period doubling bifurcations that emerge from (tsl).

When \bar{g}_K is decreased from the HH value of 36 mS/cm² the Takens-Bogdanov point in the $I \times \bar{V}_K$ plane moves towards the cusp point and past it. This agrees qualitatively with the findings of [44], but their results differ from ours in the value of \bar{g}_K for which the Takens-Bogdanov point moves past the cusp. The unfolding for the codimension three bifurcation in which cusp and Takens-Bogdanov bifurcations coincide has been analyzed by Guckenheimer [34] and Dumortier and Roussarie [16]. The geometry of the unfolding of this codimension three bifurcation can be visualized by drawing a two dimensional sphere that encloses the codimension three point in the three dimensional parameter space of the unfolding [34].

To further explore the effect of this codimension three bifurcation on the bifurcation diagrams of (HH), we decreased \bar{g}_K from the HH value of 36 mS/cm² to 12 mS/cm² and computed another bifurcation diagram in the $I \times \bar{V}_K$ plane. The new bifurcation diagram is shown in Figure 9. Among its features are a curve of double cycles (dc) that terminates at a neutral saddle loop point (nsl) instead of a double Hopf bifurcation as in the unfolding of the codimension three bifurcation. The point (nsl) does not lie on the saddle loop branch

emanating from the Takens-Bogdanov point (tb), however. Instead it ends on a saddle loop that encloses both equilibrium points. This branch of saddle loops ends on both branches of saddle-nodes at saddle node loops (snl). The branch of twisted saddle loops (tsl) that was present at the higher value of \bar{g}_K remains. It starts on the saddle-node curve at another saddle node loop. The twisted saddle loops still passes through a neutral point (tnsl) at which bifurcation curves of period doublings (pd) and doubled saddle loops (dsl) originate. Our proposed bifurcation diagrams for (HH) near the cusp points appear to be compatible with the unfolding of the Takens-Bogdanov cusp codimension three bifurcation, though the diagrams drawn here are sufficiently far from the codimension three bifurcation that significant differences with its unfolding exist.

The intent of this rapid tour of the complicated dynamics of a realistic biological model was to draw attention to the interplay between theory and numerical exploration. Since many regions in the parameter space are very small, the theory helps to guide the exploration to discover the correct bifurcation diagram.

6 The Effects of Symmetry

In the previous sections, non-generic bifurcation has arisen in multiparameter families of vector fields and is a codimension two, or higher, phenomenon. Non-generic bifurcation is often encountered in the real world as a result of symmetry and in this section we discuss the bifurcation of symmetric vector fields.

Within a generic one parameter family of vector fields, $\dot{x} = f_\lambda(x)$, bifurcations of equilibria are either saddle-node bifurcations, when a single eigenvalue passes through 0, or Hopf bifurcations, when a pair of complex conjugate eigenvalues cross the imaginary axis. These are both well understood [36], but with symmetry, generic bifurcation can be much more complicated. One of our goals has been to explore how complex local bifurcation with symmetry can be.

We first make a few definitions. Let G be a finite subgroup of $O(n)$ acting on R^n . An equation $\dot{x} = f(x)$ is G -equivariant or symmetric if

$$f(gx) = g \circ f(x) \text{ for all } g \in G .$$

For a fixed group G , we wish to study generic bifurcation within the class of G -equivariant vector fields.

We now make two assumptions on the group action. The first is that the action of G is absolutely irreducible. This means that the only matrices which commute with G are scalar multiples of the identity. The second is that the action of G is fixed point free: the only point fixed by G is the origin. These assumptions have two consequences for G -equivariant vector fields. The first is that the origin is always an equilibrium point of a G -equivariant vector field, since

$$f(0) = f(g0) = gf(0) \Rightarrow f(0) = 0 .$$

The second consequence is that the linearization at the origin is a multiple of the identity. This follows from the calculations:

$$\begin{aligned} D(f \circ g)|_0 &= Df|_{g(0)} g = Df|_0 g \\ \text{and } D(f \circ g)|_0 &= D(g f)|_0 = g Df|_0 \end{aligned}$$

Because $Df|_0$ commutes with all $g \in G$ and G is absolutely irreducible, $Df|_0$ must be a scalar multiple of the identity. We may now state the following:

Theorem 6.1 *Let G be fixed point free and absolutely irreducible and let $\dot{x} = f_\lambda(x)$ be a one-parameter family of G -equivariant vector fields. If the origin undergoes a bifurcation with one zero eigenvalue for $\lambda = \lambda_0$, then the linearization at the origin is given by $Df_\lambda|_{(0, \lambda_0)} = 0$. In other words, all the eigenvalues must pass through zero simultaneously.*

This degenerate linearization occurs as a codimension one phenomenon due to the symmetry of the problem. We wish to analyze the bifurcations at the origin, but the possibilities are not clear and there are still many restrictions due to the equivariance.

To study the bifurcation in an analogous fashion as for the non-symmetric case, we will compute a normal form by computing a Taylor series at the origin:

$$f_\lambda(x) = \sum_{i=1}^{\infty} P_i(x) .$$

Each P_i is a homogeneous, degree i , G -equivariant. The P_i are not always easy to calculate and we are led to the study of polynomial invariants and equivariants which combines elements of combinatorial theory and modern commutative algebra [33, 64], but we shall not delve into this topic in this paper.

We shall now study a simple example: D_4 acting on R^2 , which may be thought of as the symmetry of the square in the plane. Generators for this action are given by

$$\begin{pmatrix} 1 & 0 \\ 0 & -1 \end{pmatrix} \text{ and } \begin{pmatrix} 0 & 1 \\ 1 & 0 \end{pmatrix} ,$$

and it is easy to show that this action is fixed point free and absolutely irreducible. We look at the degree three power series expansion at the origin:

$$\begin{aligned} \dot{x} &= \lambda x + ax^3 + bxy^2 \\ \dot{y} &= \lambda y + ay^3 + bx^2y \end{aligned}$$

As λ passes through 0, the origin changes stability, but what else happens in the process? We can get some additional information from looking at subgroups of G and fixed point subspaces.

If $H \subset G$, then we define the fixed point subspace of the subgroup H by

$$\text{Fix}(H) = \{x \in R^n \text{ such that } hx = x \text{ for all } h \in H\}.$$

Fixed point subspaces are important because they are invariant under the flow. This is easy to see because if $x \in \text{Fix}(H)$, then $f(x) = f(hx) = hf(x)$ so $f(x) \in \text{Fix}(H)$, i.e., the vector field on $\text{Fix}(H)$ is tangent to $\text{Fix}(H)$. The fixed point subspaces for the example are the axes of symmetry plus the trivial ones: the origin and all of R^2 .

To explain bifurcation in some of the fixed point subspaces, Cicogna and Vanderbauwhede formulated the following lemma:

Lemma 6.2 (*The Fixed Point Branching Lemma*) [33] *If V is a one-dimensional fixed point subspace, then there is a branch of solutions in V in $R^n \times R$ that pass through $(0, 0)$ and is part of a generic bifurcation.*

For the D_4 example, this means that on the axes of symmetry there are pitchfork bifurcations. For this simple problem, we may verify this result by explicitly computing the equilibrium points which are given by:

$$\begin{aligned} & (0, 0) \\ & (\pm\sqrt{\frac{-\lambda}{a}}, 0), (0, \pm\sqrt{\frac{-\lambda}{a}}) \\ & (\pm\sqrt{\frac{-\lambda}{a+b}}, \pm\sqrt{\frac{-\lambda}{a+b}}) \end{aligned}$$

So if $a < 0$ and $a + b < 0$, then as λ passes through zero, eight new equilibrium points are created. It is typical behavior to get multiple equilibrium points in equivariant bifurcations and a substantial theory has been developed by M. Field [17], M. Golubitsky [33] and others. This work, based on group theory and singularity theory, can give information about bifurcation to equilibrium points, period orbits and quasiperiodic orbits. However, this is a far from complete categorization of the behavior which may be obtained from more complicated group actions.

Now consider the action of a group G on R^3 generated by

$$\begin{pmatrix} -1 & 0 & 0 \\ 0 & 1 & 0 \\ 0 & 0 & 1 \end{pmatrix} \text{ and } \begin{pmatrix} 0 & 1 & 0 \\ 0 & 0 & 1 \\ 1 & 0 & 0 \end{pmatrix}.$$

The action is fixed point free, absolutely irreducible and, a few short calculations show, the degree three equivariant vector field has the form:

$$\begin{aligned} \dot{x}_1 &= (\lambda + a_1x_1^2 + a_2x_2^2 + a_3x_3^2)x_1 \\ \dot{x}_2 &= (\lambda + a_1x_2^2 + a_2x_3^2 + a_3x_1^2)x_2 \\ \dot{x}_3 &= (\lambda + a_1x_3^2 + a_2x_1^2 + a_3x_2^2)x_3 \end{aligned} \tag{2}$$

One of the consequences of the symmetry is the invariance of both the coordinate axes and the coordinate planes. Guckenheimer and Holmes [35] observed that this system of equations has structurally stable heteroclinic cycles for open regions of the parameter space.

Theorem 6.3 *If either $a_3 < a_1 < a_2 < 0$ or $a_2 < a_1 < a_3 < 0$ and $2a_1 > a_2 + a_3$ then Equations 2 have attracting heteroclinic cycles for $\lambda > 0$ and a globally attracting equilibrium at the origin for $\lambda \leq 0$.*

This theorem essentially follows from examining the flow in the invariant coordinate planes. The consequence is that within families of G -equivariant vector fields there are generic one parameter bifurcations from an attracting equilibrium point to structurally stable attracting limit cycles. We continue to study more complicated symmetry groups in an attempt to

discover how complicated post bifurcation behavior can be. The answer is that a stable equilibrium point can bifurcate directly to a chaotic attractor of small amplitude [38].

Consider the action of \bar{G} on R^4 generated by

$$\begin{pmatrix} -1 & 0 & 0 & 0 \\ 0 & 1 & 0 & 0 \\ 0 & 0 & 1 & 0 \\ 0 & 0 & 0 & 1 \end{pmatrix} \text{ and } \begin{pmatrix} 0 & 1 & 0 & 0 \\ 0 & 0 & 1 & 0 \\ 0 & 0 & 0 & 1 \\ 1 & 0 & 0 & 0 \end{pmatrix}$$

as studied by Field and Swift [19]. The cubic truncation of the general \bar{G} -equivariant vector field is given by

$$\begin{aligned} \dot{x}_1 &= (\lambda + a_1 x_1^2 + a_2 x_2^2 + a_3 x_3^2 + a_4 x_4^2) x_1 \\ \dot{x}_2 &= (\lambda + a_1 x_2^2 + a_2 x_3^2 + a_3 x_4^2 + a_4 x_1^2) x_2 \\ \dot{x}_3 &= (\lambda + a_1 x_3^2 + a_2 x_4^2 + a_3 x_1^2 + a_4 x_2^2) x_3 \\ \dot{x}_4 &= (\lambda + a_1 x_4^2 + a_2 x_1^2 + a_3 x_2^2 + a_4 x_3^2) x_4 \end{aligned}$$

First observe that if all the $a_i = -1$, then in the flow of the vector field, for $\lambda < 0$ the origin is globally attracting, and for $\lambda > 0$ there is an invariant attracting sphere of radius $\sqrt{\lambda}$. The sphere is normally hyperbolic. If the a_i are close to -1 , then there will be an invariant topological 3-sphere in the post bifurcation flow (The Invariant Sphere Theorem [18]).

We may now ask about the dynamics on the invariant 3-sphere. We rescale the phase space variables by $\sqrt{\lambda}$ and the independent variable by $1/\lambda$ to blow up the sphere, which is equivalent to setting $\lambda = 1$ in the above equations. Varying the parameters a_i , we study the flow on the sphere realizing that all the dynamics on the sphere represent possible post bifurcation behavior of the vector field. Structurally stable objects give persistent post bifurcation behavior for \bar{G} -equivariant families. All indications imply that this system has no chaotic behavior, but consider $G \subset \bar{G}$, the elements of the group G which are orientation preserving. A new term must be added to the equivariant vector field which results in

$$\begin{aligned} \dot{x}_1 &= (\lambda + a_1 x_1^2 + a_2 x_2^2 + a_3 x_3^2 + a_4 x_4^2) x_1 + e x_2 x_3 x_4 \\ \dot{x}_2 &= (\lambda + a_1 x_2^2 + a_2 x_3^2 + a_3 x_4^2 + a_4 x_1^2) x_2 - e x_1 x_3 x_4 \\ \dot{x}_3 &= (\lambda + a_1 x_3^2 + a_2 x_4^2 + a_3 x_1^2 + a_4 x_2^2) x_3 + e x_1 x_2 x_4 \\ \dot{x}_4 &= (\lambda + a_1 x_4^2 + a_2 x_1^2 + a_3 x_2^2 + a_4 x_3^2) x_4 - e x_1 x_2 x_3 \end{aligned}$$

The geometry associated with this group action appears to be very rich and was first examined by Guckenheimer and Worfolk [38]. For $a_i \approx -1$ and $\lambda > 0$, there is an invariant, attracting, topological sphere in the flow on which we wish to study the dynamics. Also, as in the earlier examples, there are structurally stable heteroclinic cycles given by the intersection of the invariant sphere and the invariant $x_i - x_{i+1}$ orthogonal coordinate planes.

The geometry associated with this group action appears to be very rich. We may think of objects as bifurcating from the heteroclinic cycles as they are broken by the introduction of fixed points in the cycles. A numerical study reveals unmistakable signs of chaotic behavior: period doubling cascades and Šilnikov homoclinic orbits. This leads to the conclusion that the flow on the invariant sphere can contain chaotic attractors. All hyperbolic invariant

sets are possible post bifurcation behavior, hence we can expect to bifurcate directly from a trivial equilibrium to a chaotic attractor of small amplitude. We are currently applying the techniques presented for the analysis of homoclinic bifurcations to the task of analytically proving the existence of chaotic behavior in a neighborhood of the heteroclinic cycles. This would verify the following conjecture formulated from the numerical exploration.

Conjecture 6.4 *There is an open region \mathcal{U} in the space of one parameter families of vector fields on R^4 equivariant with respect to G , such that $X_\lambda \in \mathcal{U}$ implies that a bifurcation of the trivial equilibrium point occurs in X_λ at $\lambda = \lambda_0$ that produces “instant chaos”. This means that if U is a neighborhood of the origin in R^4 , then there is an $\epsilon > 0$ such that X_λ has a chaotic hyperbolic invariant set contained in U for $0 < \lambda - \lambda_0 < \epsilon$.*

7 Acknowledgements

The authors would like to thank Allen Back for his help with the computation of two-dimensional manifolds and Mark Myers for his help with the section on Hopf bifurcations.

8 Captions for Figures

Figure 1: Evolve the stable manifold of p using geodesic curves.

Figure 2: The stable manifold of the origin in the Lorenz system projected onto the x-z plane.

Figure 3: Depiction of section of $W^{s+} \cap W^{u+}$ for typical homoclinic orbits.

Figure 4: Unifocal and bifocal homoclinic orbits.

Figure 5: Bifurcation diagram for an untwisted resonant homoclinic orbit.

Figure 6: Bifurcation diagrams for twisted resonant homoclinic orbit.

Figure 7: Return maps for the planar gluing bifurcation.

Figure 8: Bifurcation diagram for the Hodgkin and Huxley equations.

Figure 9: Bifurcation diagram for the Hodgkin and Huxley equations, with $\bar{g}_K = 12 \text{ mS/cm}^2$.

References

- [1] F. Argoul, A. Arneodo, and P. Richetti. Experimental evidence for homoclinic chaos in the Belousov-Zhabotinskii reaction. *Phys. Lett. A*, 120(6):269–275, 1987.
- [2] V. I. Arnold. *Geometrical Methods in the Theory of Ordinary Differential Equations*. Springer-Verlag, New York, 1988.
- [3] A. Back, J. Guckenheimer, M. Myers, F. Wicklin, and P. Worfolk. dstool: Computer assisted exploration of dynamical systems. *Notices Amer. Math. Soc.*, 39(4):303–309, 1992.
- [4] C. Baesens, J. Guckenheimer, S. Kim, and R. Mackay. Three coupled oscillators: Mode-locking, global bifurcations and toroidal chaos. *Phys. D*, 49:387–475, 1991.
- [5] L. Belyakov. Bifurcation of systems with homoclinic curve of a saddle-focus with saddle quantity zero. *Mat. Zametki*, 36(5):681–689, 1985.
- [6] M. Benedicks and L. Carleson. The dynamics of the Hénon map. *Ann. of Math.*, 133:73–169, 1991.
- [7] W. J. Beyn. The numerical computation of connecting orbits in dynamical systems. *IMA J. Numer. Anal.*, 9:169–181, 1990.
- [8] M. Bosch and C. Simo. Attractors in a Šilnikov-Hopf scenario and a related one-dimensional map. *Phys. D*, 62:217–229, 1993.
- [9] S.-N. Chow, B. Deng, and B. Fiedler. Homoclinic bifurcation at resonant eigenvalues. *J. Dynamics Differential Equations*, 2(2):177–244, 1990.
- [10] S.-N. Chow, B. Deng, and D. Terman. The bifurcation of homoclinic and periodic orbits from two heteroclinic cycles. *SIAM J. Math. Anal.*, 21(1):179–204, 1990.
- [11] S. N. Chow and X. B. Lin. Bifurcation of a homoclinic orbit with a saddle-node equilibrium. *Differential Integral Equations*, 3:435–466, 1990.
- [12] B. Deng. Homoclinic bifurcations with nonhyperbolic equilibria. *SIAM J. Math. Anal.*, 21(3):693–720, 1990.
- [13] B. Deng. The bifurcations of countable connections from a twisted homoclinic loop. *SIAM J. Math. Anal.*, 22(3):653–679, 1991.
- [14] B. Deng. Homoclinic twisting bifurcation and cusp horseshoe maps. Preprint, Dec. 1991.
- [15] M. H. Dulac. Sur les cycles limites. *Bull. Soc. Math. Anal.*, 51:45–188, 1923.
- [16] F. Dumortier, R. Roussarie, and J. Sotomayor. Generic 3-parameter families of vector fields on the plane, unfolding a singularity with nilpotent linear part. The cusp case of codimension 3. *Ergodic Theory Dynamical Systems*, 7:375–413, 1987.

- [17] M. Field. Equivariant dynamics. *Contemp. Math.*, 56:69–96, 1986.
- [18] M. Field. Equivariant bifurcation theory and symmetry breaking. *J. Dynamics Differential Equations*, 1(4):369–421, 1989.
- [19] M. Field and J. Swift. Stationary bifurcation to limit cycles and heteroclinic cycles. *Nonlinearity*, 4:1001–1043, 1991.
- [20] A. C. Fowler and C. T. Sparrow. Bifocal homoclinic orbits in four dimensions. *Nonlinearity*, 4:1159–1182, 1991.
- [21] M. J. Friedman. Numerical analysis and accurate computation of heteroclinic orbits in the case of center manifolds. To appear in *J. Dynamics Differential Equations*, 1992.
- [22] M. J. Friedman and E. J. Doedel. Computational methods for global analysis of homoclinic and heteroclinic orbits: a case study. To appear in *J. Dynamics Differential Equations*, 1992.
- [23] A. T. Fuller. Conditions for a matrix to have only characteristic roots with negative real parts. *J. Math. Anal. Appl.*, 23:71–98, 1968.
- [24] P. Gaspard. Generation of a countable set of homoclinic flows through bifurcation. *Phys. Lett. A*, 97(1):1–4, 1983.
- [25] P. Gaspard, R. Kapral, and G. Nicolis. Bifurcation phenomena near homoclinic systems: A two-parameter analysis. *J. Statist. Phys.*, 35(5/6):697–727, 1984.
- [26] P. Gaspard and X.-J. Wang. Homoclinic orbits and mixed-mode oscillations in far-from-equilibrium systems. *J. Statist. Phys.*, 48(1):151–199, 1987.
- [27] P. Glendinning. Travelling wave solutions near isolated double-pulse solitary waves of nerve axon equations. *Phys. Lett. A*, 121:411–413, 1987.
- [28] P. Glendinning. Subsidiary bifurcations near bifocal homoclinic orbits. *Math. Proc. Cambridge Philos. Soc.*, 105:597–605, 1989.
- [29] P. Glendinning and C. Sparrow. Local and global behavior near homoclinic orbits. *J. Stat. Phys.*, 34(5/6):645–696, 1984.
- [30] P. Glendinning and C. Sparrow. T-points: A codimension two heteroclinic bifurcation. *J. Stat. Phys.*, 43(3/4):479–488, 1986.
- [31] P. Glendinning and C. Tresser. Heteroclinic loops leading to hyperchaos. *J. Physique Lett.*, 46(8):347–352, 1985.
- [32] M. Golubitsky and V. Guillemin. *Stable Mappings and Their Singularities*. Springer-Verlag, New York, 1973.
- [33] M. Golubitsky, I. Stewart, and D. Shaeffer. *Singularities and Groups in Bifurcation Theory*, volume II. Springer-Verlag, New York, 1988.

- [34] J. Guckenheimer. Multiple bifurcation problems for chemical reactors. *Phys. D*, 20:1–20, 1986.
- [35] J. Guckenheimer and P. Holmes. Structurally stable heteroclinic cycles. *Math. Proc. Cambridge Philos. Soc.*, 103:189–192, 1988.
- [36] J. Guckenheimer and P. J. Holmes. *Nonlinear Oscillations, Dynamical Systems, and Bifurcations of Vector Fields*. Springer-Verlag, New York, 1983.
- [37] J. Guckenheimer and R. Williams. Structural stability of Lorenz attractors. *Publ. Math. IHES*, 50:59–72, 1979.
- [38] J. Guckenheimer and P. Worfolk. Instant chaos. *Nonlinearity*, 5:1211–1222, 1992.
- [39] B. D. Hassard and L.-J. Shiau. Isolated periodic solutions of the Hodgkin-Huxley equations. *J. Theoret. Biol.*, 136:267–280, 1989.
- [40] M. Hénon. A two-dimensional mapping with a strange attractor. *Comm. Math. Phys.*, 50:69–77, 1976.
- [41] P. Hirschberg and E. Knobloch. Silnikov-Hopf bifurcation. *Phys. D*, 62:202–216, 1993.
- [42] A. L. Hodgkin and A. F. Huxley. Current carried by sodium and potassium ions through the membrane of the giant axon of loligo. *J. Physiology*, 116:449–472, 1952.
- [43] A. L. Hodgkin and A. F. Huxley. A quantitative description of membrane current and its applications to conduction and excitation in nerve. *J. Physiology*, 117:500–544, 1952.
- [44] A. V. Holden, M. A. Muhamad, and A. K. Schierwagen. Repolarizing currents and periodic activity in nerve membrane. *J. Theoret. Neurobiol.*, 4:61–71, 1985.
- [45] P. Glendinning J. M. Gambaudo and C. Tresser. Collage de cycles et suites de Farey. *C. R. Acad. Sci. Paris*, 299:711–714, 1984.
- [46] H. B. Keller. Numerical solution of bifurcation and nonlinear eigenvalue problems. In P. Rabinowitz, editor, *Applications of Bifurcations Theory*, pages 359–384. Academic Press, 1977.
- [47] H. Kokubu. Homoclinic and heteroclinic bifurcations of vector fields. *Japan J. Appl. Math*, 5:455–501, 1988.
- [48] I. S. Labouriau. Degenerate Hopf bifurcation and nerve impulse, Part II. *SIAM J. Math. Anal.*, 20:1–12, 1989.
- [49] R. Loos. Generalized polynomial remainder sequences. In G.E Collins B. Buchberger and R. Loos, editors, *Computer Algebra - Symbolic and Algebraic Computation*, pages 115–137. Springer-Verlag, 1982.
- [50] E. N. Lorenz. Deterministic non-periodic flow. *J. Atmospheric Sci.*, 20:130–141, 1963.

- [51] V. Luk'yanov. Bifurcations of dynamical systems with a saddle-point-separatrix loop. *J. Differential Equations*, 18:1049–1059, 1983.
- [52] L. Mora and M. Viana. Abundance of strange attractors. Preprint, 1991.
- [53] J. Palis and W. de Melo. *Geometric Theory of Dynamical Systems*. Springer-Verlag, New York, 1982.
- [54] R. Richetti, F. Argoul, and A. Arneodo. Type-II intermittency in a periodically driven nonlinear oscillator. *Phys. Rev. A*, 34(1):726–729, 1986.
- [55] J. Rinzel and R. N. Miller. Numerical solutions of the Hodgkin-Huxley equations. *Math. Biosci.*, 49:27–59, 1980.
- [56] S. Schecter. The saddle-node separatrix-loop bifurcation. *SIAM J. Math. Anal.*, 18(4):1142–1156, 1987.
- [57] S. Schecter. Simultaneous equilibrium and heteroclinic bifurcation of planar vector fields via the Melnikov integral. *Nonlinearity*, 3:79–99, 1990.
- [58] S. Schecter. C^1 singularity theory and heteroclinic bifurcation with a distinguished parameter. *J. Differential Equations*, 99:306–341, 1992.
- [59] S. Schecter. Numerical computation of saddle-node homoclinic bifurcation points. to appear in SIAM J. Numer. Anal., 1993.
- [60] L. P. Silnikov. A case of the existence of a countable number of periodic motions. *Soviet Math. Dokl.*, 6:163–166, 1965.
- [61] L. P. Silnikov. The existence of a denumerable set of periodic motions in four-dimensional space in an extended neighborhood of a saddle-focus. *Soviet Math. Dokl.*, 8(1):54–58, 1967.
- [62] L. P. Silnikov. On the generation of a periodic motion from trajectories doubly asymptotic to an equilibrium state of saddle type. *Math. USSR-Sb.*, 6(3):427–438, 1968.
- [63] L. P. Silnikov. A contribution to the problem of the structure of an extended neighborhood of a rough equilibrium of saddle-focus type. *Math. USSR-Sb.*, 10(1):91–102, 1970.
- [64] R.P. Stanley. Invariants of finite groups and their applications to combinatorics. *Bull. Amer. Math. Soc.*, 1(3):475–511, 1979.
- [65] D. Terman. The transition from bursting to continuous spiking in excitable membrane models. *J. Nonlinear Science*, 2(2):135–182, 1992.
- [66] C. Tresser. About some theorems by L.P. Šilnikov. *Ann. Inst. H. Poincaré Sect. A*, 40(4):441–461, 1984.

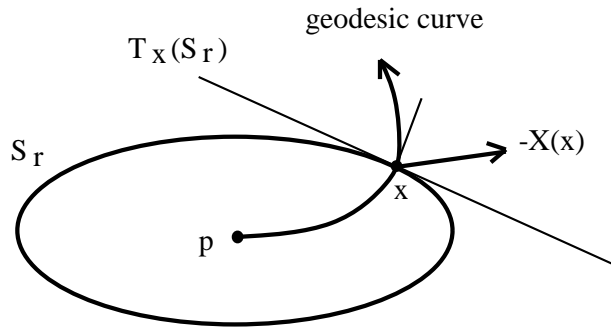


Figure 1: Evolve the stable manifold of p using geodesic curves.

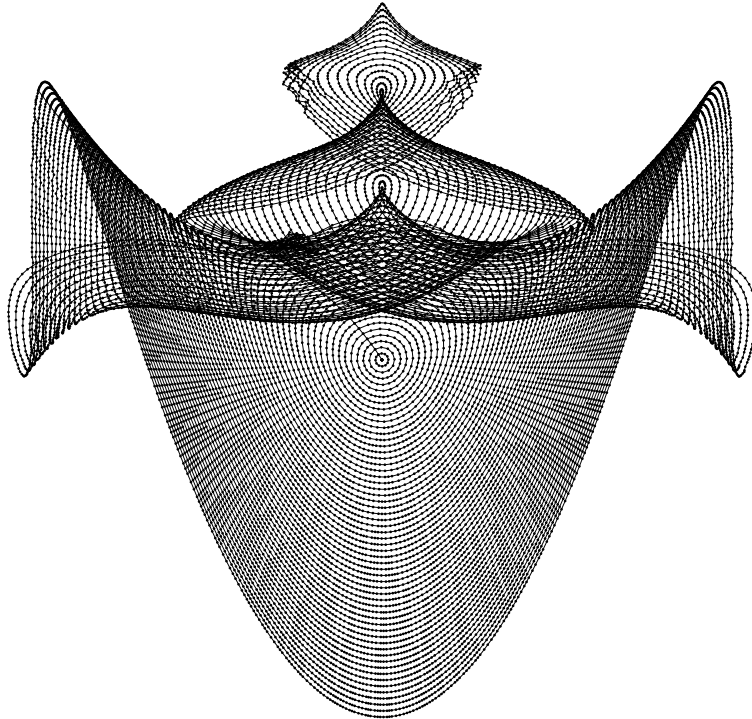


Figure 2: The stable manifold of the origin in the Lorenz system projected onto the x - z plane.

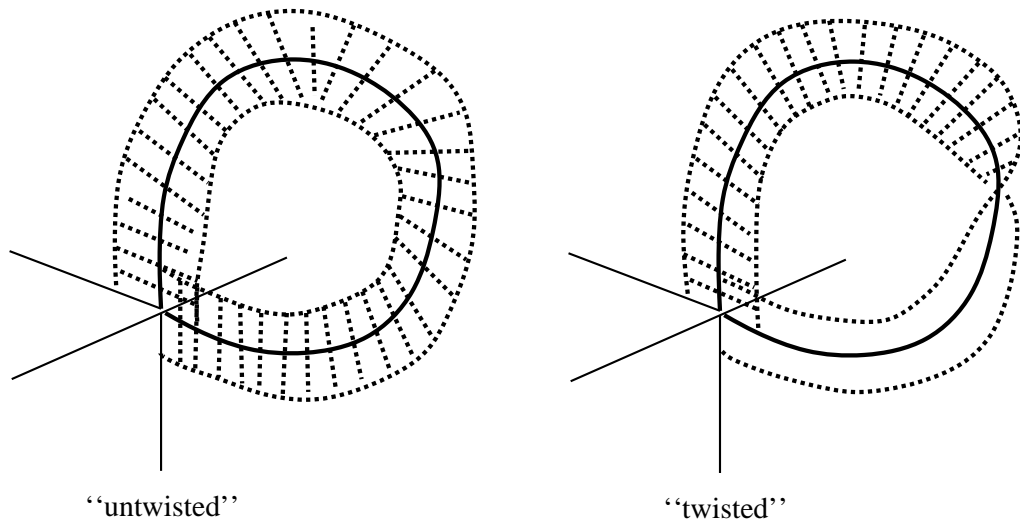


Figure 3: Depiction of section of $W^{s+} \cap W^{u+}$ for typical homoclinic orbits.

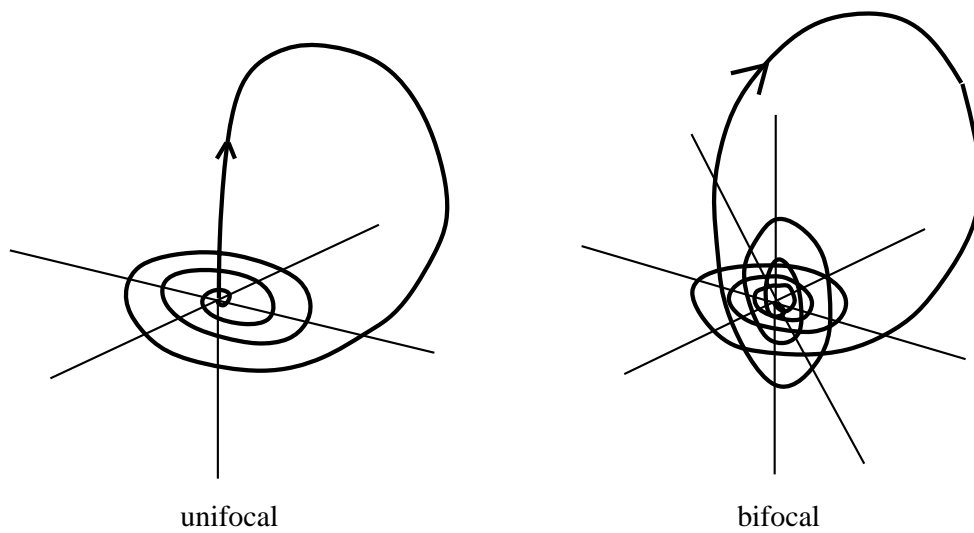


Figure 4: Unifocal and bifocal homoclinic orbits.

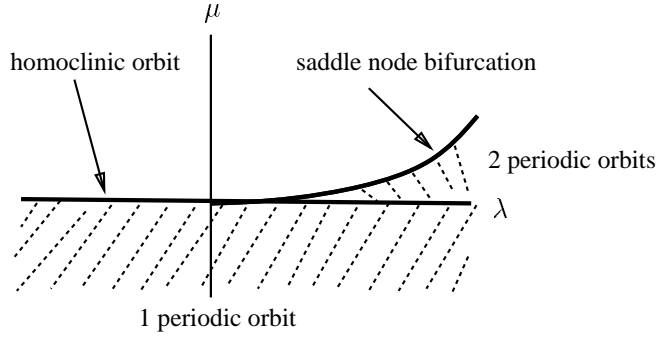


Figure 5: Bifurcation diagram for an untwisted resonant homoclinic orbit.

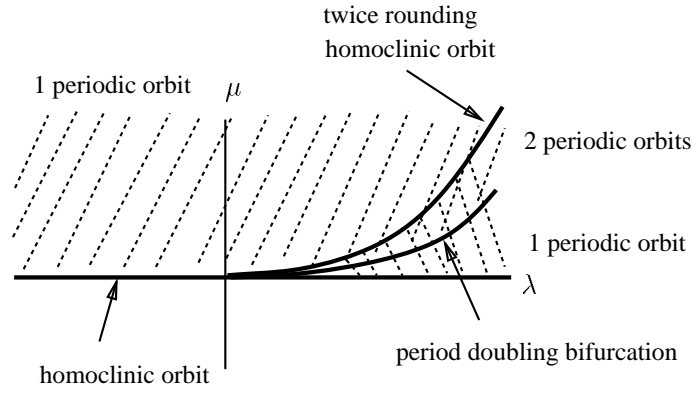


Figure 6: Bifurcation diagrams for a twisted resonant homoclinic orbit.

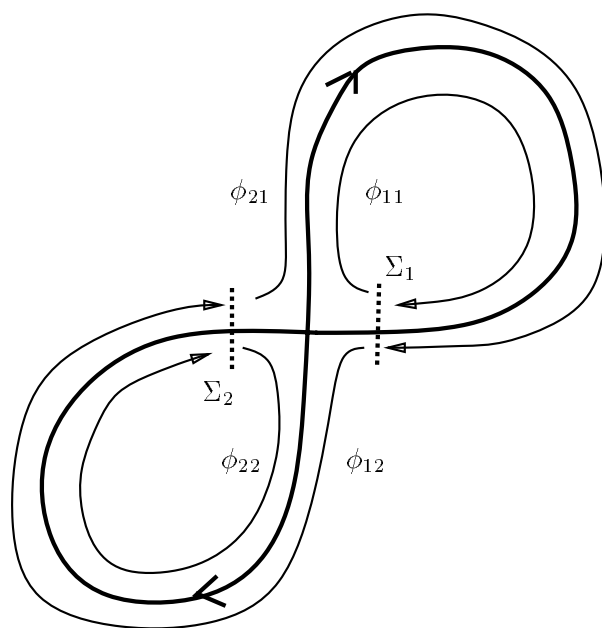


Figure 7: Return maps for the planar gluing bifurcation.

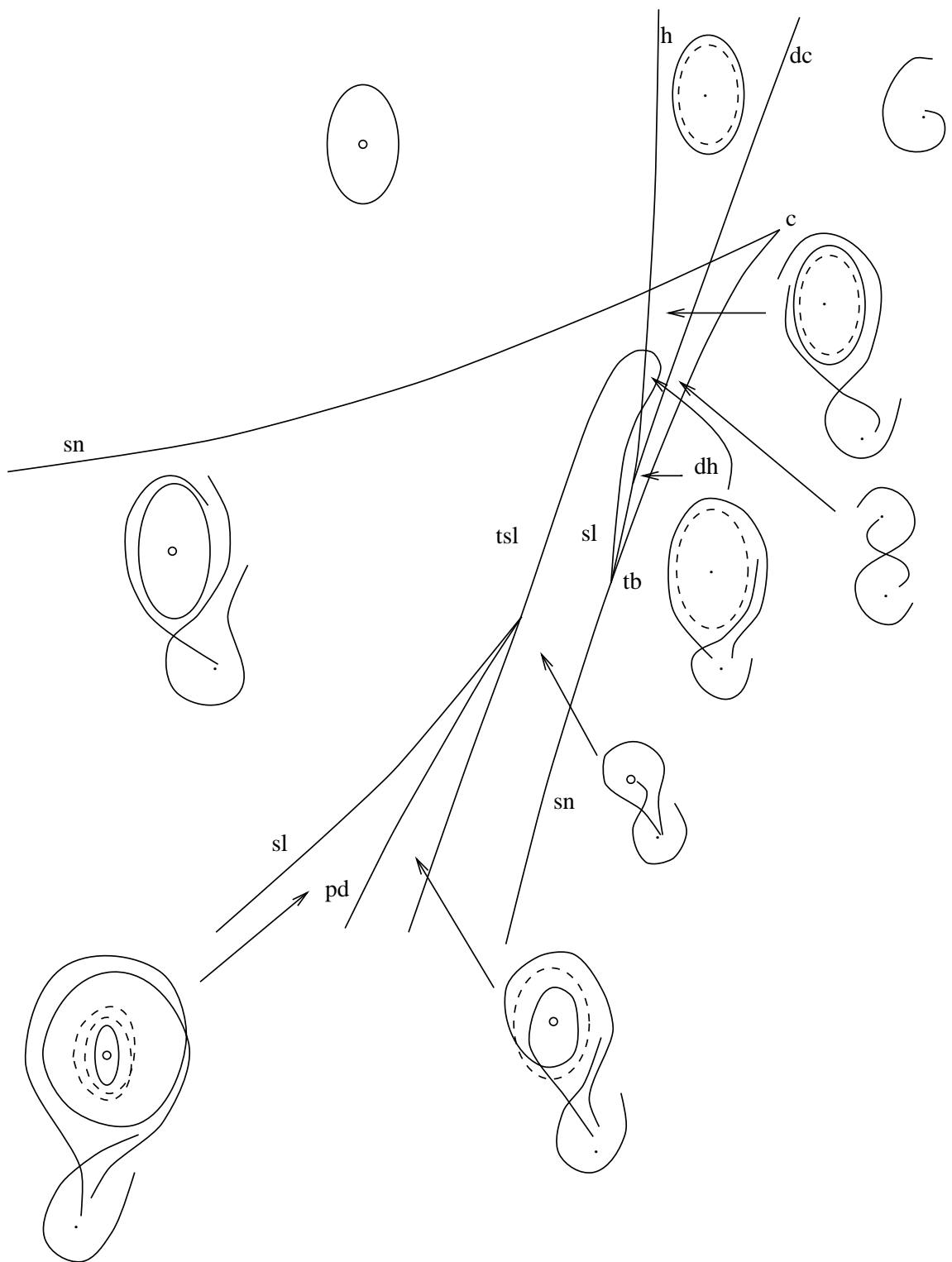


Figure 8: Bifurcation diagram for the Hodgkin and Huxley equations.

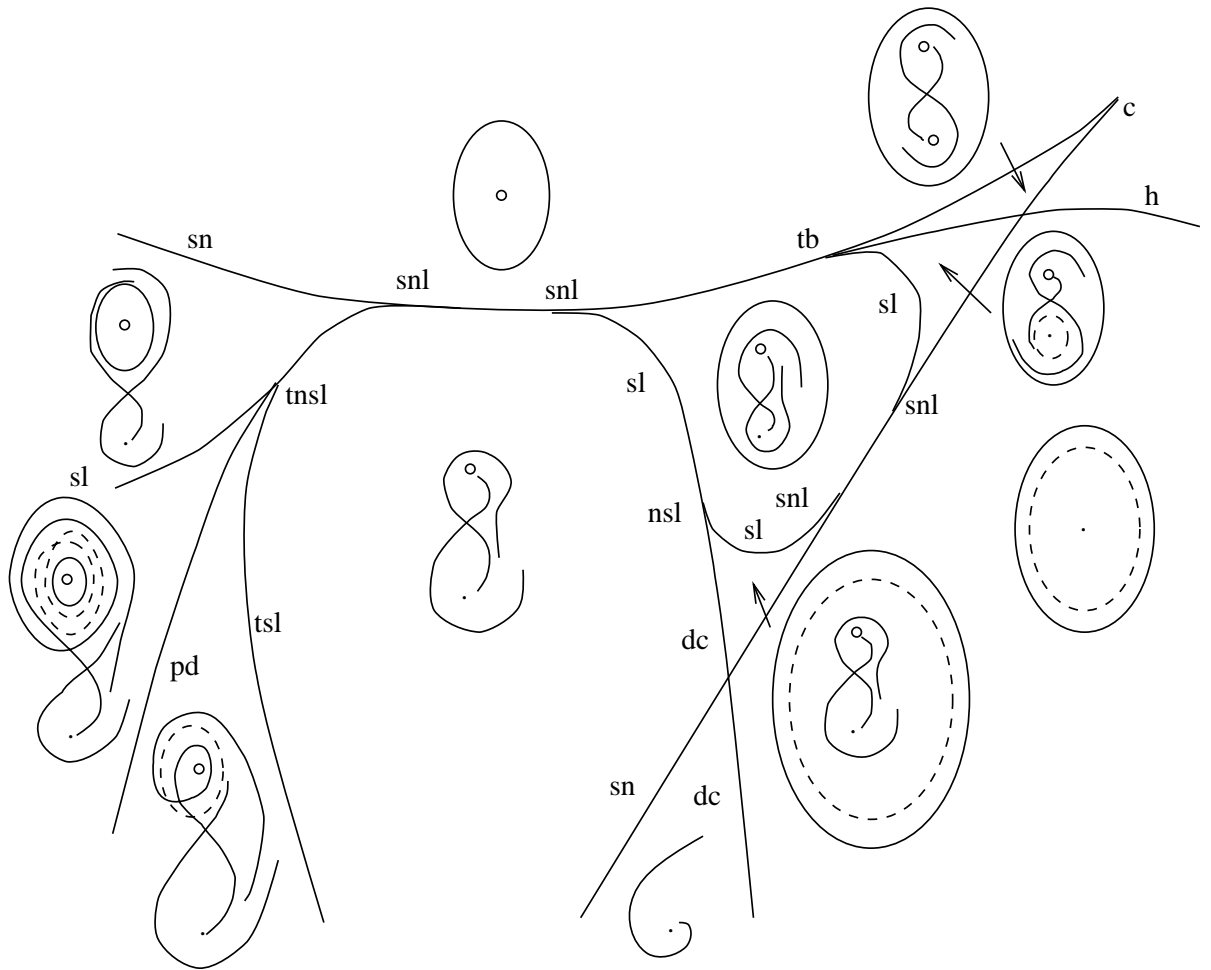


Figure 9: Bifurcation diagram for the Hodgkin and Huxley equations, with $\bar{g}_K = 12 \text{ mS/cm}^2$.